https://doi.org/10.5194/egusphere-2026-2745
Preprint. Discussion started: 27 May 2026

Marine Organic Aerosols Reflect Ecosystem Variability from Phytoplankton Functional Types to Micronekton

Emmanuel Chevassus[1], Vaios Moschos[1], Kirsten N. Fossum[1], Lu Lei[1], Liz Coleman[1], Dagmar B. Stengel[1], Vignesh Prabhu[1], Wei Xu[1+], Darius Ceburnis[1], Colin O' Dowd[1], Jurgita Ovadnevaite[1]

[1] School of Natural Sciences, Ryan Institute's Centre for Climate and Air Pollution Studies, University of Galway, H91 TK33, Co. Galway, Ireland

[+] Now at Institute of Urban Environment, Chinese Academy of Sciences, Xiamen 361021

Correspondence to: Jurgita Ovadnevaite (jurgita.ovadnevaite@universityofgalway.ie)

Abstract

Marine organic aerosols remain a major source of uncertainty in aerosol cloud–climate interactions, in part because marine ecosystem structure and biological drivers are often represented in overly simplified terms, typically reduced to bulk chlorophyll-*a*. Here, a full year of high-resolution aerosol mass spectrometry measurements at Mace Head (west coast of Ireland) is combined with HYSPLIT air-masses exposure metrics and gap-free phytoplankton functional type (PFT) fields to explore influences on primary marine organic aerosol (PMOA) and methane sulphonic acid (MSA). During the spring-summer diatom climax, PMOA correlates with dominant bloom taxa (R=0.65-0.70) and micronekton (R=0.55), with rapid 1-3 day responses and secondary maxima at ~25 days, consistent with early labile release and later lysis/grazing. During that same phase, MSA also showed a lagged responses to both PFT and micronekton reflecting delayed DMS production and oxidation. However, comparable phytoplankton air-mass exposure in the late summer of that same year (i.e. early depletion phase) did not reproduce such high correlations, with time-scale analyses indicating weakened coupling at warmer sea-surface temperatures despite moderately stronger winds. These results imply that structured ecosystem composition and physical forcing both contribute to cross-basin seasonal differences in marine organic aerosols formation. This motivates future research vessel campaigns and mesocosm experiments to explicitly manipulate PFT interactions and air-sea physics.

Keywords: submicron organic aerosols, sea spray organics, high-resolution aerosol mass spectrometry, positive matrix factorisation, phytoplankton functional types, micronekton.

https://doi.org/10.5194/egusphere-2026-2745
Preprint. Discussion started: 27 May 2026

1 Introduction

The Earth's energy imbalance has more than doubled in recent decades, driven primarily by anthropogenic greenhouse-gas emissions, with additional contributions from declining planetary albedo linked to sea-surface temperature changes and aerosol-cloud feedback (Mauritsen *et al.,* 2025). Anthropogenic effective radiative forcing (RF) since 1750 is estimated at 2.72 W m^{-2} [1.96 to 3.48 W m^{-2}] while aerosol-radiation interactions contribute -0.22 W m^{-2} [-0.47 to 0.04 W m^{-2}] and submicron aerosol-cloud indirect interactions -0.84 W m^{-2} [-1.45 to -0.25 W m^{-2}], reflecting substantial uncertainties from aerosol-cloud interactions that remain poorly constrained in Intergovernmental Panel on Climate Change (IPCC) reports (Forster *et al.,* 2023). Beyond these anthropogenic influences, growing evidences also suggest that natural marine sources play a larger role than previously thought in modulating global RF, emphasising the urgent need for improved observational and process-level understanding (Hodshire *et al.,* 2019; Sellegri *et al.,* 2024). Concurrently, climate change increasingly modifies ocean biogenic activity and air-sea transfer physics (Hong *et al.,* 2025; Law and Miller, 2025), thereby altering the global pool of marine aerosols including sea salt, oxidised secondary organic aerosol, methane sulphonic acid (MSA), and primary marine organic aerosol (PMOA) that seed low-level marine clouds.

PMOA is produced by breaking waves as bubbles containing biogenic sea spray burst at the ocean´s surface (O'Dowd *et al.,* 2004; Ovadnevaite *et al.,* 2014; Villermaux *et al.,* 2022). As a result of measurements and modelling propagating uncertainties, global PMOA fluxes are not yet fully resolved with estimates ranging from 9 to 29 Tg-$year^{-1}$ (Burrows *et al.,* 2022; Leon-Marcos *et al.,* 2024) while global PMOA contribution to indirect RF remains highly uncertain in both magnitude and spatial variability (Burrows *et al.,* 2022; Partanen *et al.,* 2014). In contrast, total sea spray aerosol emissions, dominated by (super-micron) sea salt, are much larger (≈2,000-10,000 Tg yr^{-1}). Despite their far smaller mass, marine organic aerosols are known to exert a disproportionate influence on cloud-forming properties of marine aerosols, driven by amphiphilic biopolymers that suppress droplet surface tension, and facilitate water uptake during activation across successive phytoplankton bloom stages (Kaluarachchi *et al.,* 2022; Kawana *et al.,* 2022; Ovadnevaite *et al.,* 2011).

Conversely, MSA arises from phytoplankton-derived dimethylsulphoniopropionate (DMSP), cleaved by algal and bacterial enzymes to yield dimethyl sulphide (DMS) which, once ventilated, is oxidised via multi-oxidant pathways (such as OH, NO_3 or halogens) to form MSA and other sulphur species (Goss and Kroll, 2024; Wang *et al.,* 2024). DMS largely dominates the global biogenic sulphur budget and accounts for most of natural sulphur emissions over oceans (Jackson and Gabric, 2022). Globally, DMS burden estimates range from 7.5 Gg S yr^{-1} (Fung *et al.,* 2021) to 40 Gg S yr^{-1} (Cala *et al.,* 2023) and ~20.3 Tg C yr^{-1} (Hulswar *et al.,* 2022), with estimated radiative cooling effects ranging from -1.69 W m^{-2} to -2.3 W m^{-2} (Fiddes *et al.,* 2018). Conversely, MSA contributes only weakly to radiative forcing (Hodshire *et al.,* 2019) but provides a direct tracer of marine biogenic sulphur and DMS oxidation, with

https://doi.org/10.5194/egusphere-2026-2745
Preprint. Discussion started: 27 May 2026

implications for particle formation and growth to cloud condensation nuclei (CCN) relevant sizes (Rosati *et al.,* 2022; Wollesen de Jonge *et al.,* 2021).

Although links between phytoplankton communities and marine aerosols have been demonstrated across multiple studies (Freney *et al.,* 2020; Schwier *et al.,* 2017; Trueblood *et al.,* 2021), the coupling remains uncertain as substantial variations in ocean physics (i.e. mesoscale eddies; Becker *et al.,* 2025) and geochemical variations in epipelagic organics (Lawler *et al.,* 2024; Lowenstein *et al.,* 2025; Seidel *et al.,* 2022) exist across seasons, years and oceanic regions.

At basin scale, these heterogeneities are commonly described using the "Longhurst" biogeochemical provinces, which partition the ocean into regions defined by temperature, turbulence, salinity, nutrient supply, light availability and ecosystem structure (Longhurst, 2010). These ecosystem contrasts imply large variability in the composition of the oceanic organic pool (encompassing a global marine carbon pool of ~662 Pg, comparable to the present atmospheric CO_2 burden; Seidel *et al.,* 2022) transferred to the atmosphere via sea spray. Consequently, the impact of these ecosystem contrasts on aerosol production remains potentially significant yet poorly constrained because of complex formation mechanisms and limited ecosystem-level understanding (Seidel *et al.,* 2022; Selden *et al.,* 2024; Sellegri *et al.,* 2021). For example, phytoplankton bloom decline is shaped by a suite of biological interactions (Lima-Mendez *et al.,* 2015) that remain completely absent from current PMOA source frameworks.

Consistent with this biological control on marine aerosols production framework, fresh phytoplankton blooms have been reported to account for over two-thirds of global PMOA mass fraction and up to ~80% in the Arctic (Beaupré *et al.,* 2019; Gu *et al.,* 2023). While isotope analysis remains a benchmark for phytoplankton-aerosol coupling, this method provides limited temporal resolution and cannot resolve specific phytoplankton sources. Hence, to advance understanding of phytoplankton-aerosol coupling, there is a need to develop a more integrative framework based on online measurements (Crocker *et al.,* 2020).

Previous studies have revealed direct associations between atmospheric measurements and diatoms (Eickhoff *et al.,* 2023; Ickes *et al.,* 2020; Thornton *et al.,* 2023a), haptophytes (Alsante *et al.,* 2025), dinoflagellates (Wieber *et al.,* 2025), *Prochlorococcus* and other prokaryotes (Dall'Osto *et al.,* 2022; Wolf *et al.,* 2019), chlorophytes (Thornton *et al.,* 2023b) and cryptophytes (Trueblood *et al.,* 2021); yet, such studies remain scarce and some PFT (e.g. pelagophytes) or commensals still remain understudied (Bar-On and Milo, 2019; Moallemi *et al.,* 2021). This work aims at responding to these challenges by using observations from the Mace Head Atmospheric Research Station, a long-term Northeast Atlantic site that frequently samples clean marine air masses influenced by regional phytoplankton activity. Here we thus combine a full year of high-resolution aerosol mass spectrometry measurements with organic aerosols source apportionment and air-mass exposure to eight phytoplankton functional types (PFTs) and micronekton to define origins and properties of PMOA and MSA.

https://doi.org/10.5194/egusphere-2026-2745
Preprint. Discussion started: 27 May 2026

2. Materials and Methods

2.1 Site Description

The Mace Head Atmospheric Research Station is strategically located on the west coast of Ireland at 53°19'N, 9°54'W in Connemara, County Galway. Positioned approximately 100 meters from the Atlantic Ocean coastline at 5-21 meters above sea level, the station provides an exceptional vantage point for atmospheric monitoring (O'Dowd *et al.,* 2014) as the peninsula is exposed to open ocean air masses mostly devoid of anthropogenic influence. These air masses, originating from a nominal clean sector (between 190° and 300°; Grigas *et al*. 2017) are predominantly steered by westerlies (**Figure S1**) ushered by the polar jet's low-pressure systems interspersed with episodes of polar or tropical influences (Ovadnevaite *et al.,* 2014b). The station is largely representative of Northern Hemisphere background conditions and is also especially useful for improving our understanding of large scale phenomena such as phytoplankton blooms (O'Dowd *et al.,* 2015) and, more generally, sea spray dynamics over the North-East Atlantic as a whole (Ovadnevaite *et al.,* 2011b; Xu *et al.,* 2022).

2.2 *In-situ* measurements

Ambient aerosol chemical composition was quantified with an Aerodyne high-resolution time-of-flight aerosol mass spectrometer (HR-ToF-AMS) operating with a 650 °C tungsten vaporizer (DeCarlo *et al.,* 2006). Submicron ambient aerosol was drawn from the community sampling in isokinetic conditions to avoid particle losses (Brockmann, 2011). AMS data processing followed the standard Igor-based procedures (SQUIRREL v1.65B and PIKA v1.25B). Detection limit (~1 ng m^{-3} for multi-hours organic aerosols blank filters), ionisation efficiency, particle velocity, inlet flow, and composition dependent collection efficiency were determined following standard methods (Drewnick *et al.,* 2009; Middlebrook *et al.,* 2012). Standard relative ionisation efficiency values were applied (Xu *et al.,* 2018). Additionally, MSA was derived by upscaling the $CH_3SO_2^+$ mesylate ion at *m/z* 78.98 as described in Ovadnevaite *et al.* (2014) such as:

$$MSA = CH_3SO_2 * 29.12 * 0.714 \quad [\mu g\ m^{-3}] \quad (1)$$

Where the numerical coefficients reflect respectively the applied HR-ToF-AMS calibration constants (including nitrate ionisation efficiency) and assumed relative ionisation efficiency for MSA.

Equivalent black carbon (eBC) mass concentrations were also measured with a multi-angle absorption photometer (MAAP, Thermo Fisher Scientific model 5012) operating at a flow rate of 10 L min^{-1} and a 5 min time resolution with optical correction as described in (Xu *et al.,* 2020). During the first half of 2018, the MAAP was used to flag pollution events while in the second half of 2018, a dual spot aethalometer (Model 33, Magee Scientific) was used instead with optical correction as described in Fossum *et al*. (2024).

https://doi.org/10.5194/egusphere-2026-2745
Preprint. Discussion started: 27 May 2026

2.3 Source apportionment

The IGOR PRO Source Finder (SoFi v9.5.2) toolkit (Canonaco *et al*. 2013) was used to run the PMF algorithm for the source apportionment. The HR-ToF-AMS error matrix (Corbin *et al.,* 2015) was generated from the PIKA (Peak Integration by Key Analysis) v1.25B software package. Cell-wise downweighing of the organic aerosol matrix was applied such that weak (signal-to-noise ratio, SNR < 2) and poor signals (signal-to-noise ratio, SNR < 0.2, including zero and negative values) were assigned proportionally larger uncertainties to limit their influence on the PMF solution. Primary marine organic aerosol was constrained using reference mass spectra by Ovadnevaite *et al.* (2011a) with a-values (Canonaco *et al.,* 2013) ranging from 0.1 to 0.9 with steps of 0.1 between 3 to 8 factors and refined a-values of 0.1 to 0.5 with steps of 0.05 for the retained 6 factors final solution (These a-value controls how much the model can deviate from the reference spectrum, with lower values enforcing tighter constraints and higher values allowing more flexibility). To evaluate the stability of the PMF solution, a bootstrap resampling approach with a total of 300 runs was applied (Crespi *et al.,* 2016; Efron, 1979). This procedure quantifies statistical uncertainty in the PMF decomposition by evaluating the stability of the resolved PMOA factor across resampled datasets, capturing variability in both its time series and mass spectral profile, as well as the associated rotational ambiguity inherent to the solutions.

2.4 Phytoplankton Functional Types and Micronekton

PFT were taken from the AI-driven Global Daily gap-free Phytoplankton Functional Type dataset (AIGD-PFT; Zhang *et al.,* 2024a). AIGD-PFT combines *in situ* HPLC (high performance liquid chromatography) pigment measurements with OC-CCI v6.0 daily reflectance from SeaWiFS, MODIS, MERIS and VIIRS, together with environmental predictors, within a deep-learning framework that produces gap-free global daily surface fields at 4 km resolution spanning 1998 to 2023. In this work, sea-surface concentrations (mg m^{-3}) of *Prochlorococcus*, other prokaryotes (i.e. excluding *Prochlorococcus*), haptophytes, pelagophytes, diatoms, dinoflagellates, cryptophytes and chlorophytes were used. All PFTs values used in this analysis were well above the approximate detection limit of the underlying HPLC training data (~0.001 mg m^{-3}), and therefore uncertainty associated with low-concentration oligotrophic waters was not considered a limitation here. For comparison, NOAA MSL12 multi-sensor DINEOF global 9 km gap-filled chlorophyll-*a* (chl-*a*) and suspended particulate matter (SPM) were also retrieved from the COASTWATCH portal (Liu and Wang, 2022).

To complement this, epipelagic (i.e. down to 1.5 × the local euphotic depth, typically ~100-200 m) micronekton biomass fields (expressed as gC. m^{-2} in seawater) were extracted from the Copernicus Marine environment GLOBAL_MULTIYEAR_BGC_001_033 product (European Union-Copernicus Marine Service, 2021). Epipelagic micronekton (e.g., fish, crustaceans and cephalopods) are active swimmers (~1-20 cm) organised into depth-stratified functional groups with diel migration and explicit behavioural dynamics. Micronekton data are available as 1/12° (~8 km) daily hindcasts from 1998 onwards, generated with Spatial Ecosystem And POpulation DYnamic Model - Lower and Mid-Trophic

https://doi.org/10.5194/egusphere-2026-2745
Preprint. Discussion started: 27 May 2026

Levels (SEAPODYM-LMTL). More specifically, micronekton are simulated as low- and mid-trophic biomass using advection-diffusion-reaction dynamics forced by ocean currents, temperature, and satellite-derived net primary productivity, with a reported mean absolute difference of ~0.44 g C m^{-2} against observations (Albernhe *et al.,* 2024).

2.5 Air masses and Exposure

The Hybrid Single-Particle Lagrangian Integrated Trajectory (HYSPLIT) model (Stein et al., 2015) was set up with monthly GDAS meteorological data and 72 h-long back trajectories were generated every hour with arrival height set to 100 m above ground level. To investigate potential source regions, the simplified Quantitative Transport Bias Analysis (SQTBA) method was used to robustly represent Gaussian plumes transport bias along air masses (Zhou *et al.,* 2019). Building on SQTBA spatial extent, meteorological and wave parameters were retrieved from the European Centre for Medium-Range Weather Forecasts (C3S, 2018) to investigate source region conditions. Variables included 10 m wind components (m s^{-1}), sea surface temperature (K), 2 m air temperature (K), significant wave height (m), and peak wave period (s). Derived quantities included seawater kinematic viscosity (m^2 s^{-1}) assuming a constant salinity of 35%, atmospheric stability (the air-sea temperature difference), wave age and the Reynolds wave number following Markuszewski *et al.,* (2024) and Ovadnevaite *et al.,* (2014).

The air masses exposure to surface ocean biology was adapted from the literature assuming that submicron aerosols are well mixed within the boundary layer with diffusion and loss relating to transport time. Exposure was set to zero for trajectories endpoint pressure falling below 850 hPa and boundary layer height values below 50 m were adjusted to a minimum of 50 m (Yan *et al.,* 2024). Values were calculated as the geometric average within a 20 km radius of each trajectory endpoint (Liu *et al.,* 2022) since ocean biological surface activity is known to follow a log-normal distribution (Campbell, 1995). To determine air masses origin, the retention times over land and marine boundary layer were determined to exclude air masses with substantial terrestrial influence or weak coupling to surface marine emissions (Yan *et al.,* 2024). Furthermore, to evaluate the influence of methodological choices on the exposure estimates, sensitivity tests were performed for both the trajectory radii and trajectory lifetime (**Figures S2-S3**). Given that fronts and eddies can move up to 50-80 km day^{-1} (Gangrade and Mangolte, 2024), radii of 20-80 km were tested and yielded consistent exposure time series, indicating limited sensitivity to buffer size. Similarly, varying the back-trajectory duration from 24 h to 72 h showed broad consistency in the exposure signal with inter Pearsons's correlations always exceeding 0.7.

https://doi.org/10.5194/egusphere-2026-2745
Preprint. Discussion started: 27 May 2026

2.6 Time series and Lags Analysis

Changepoints (i.e. blooms regime shifts) were identified in phytoplankton exposure time series using the *EnvCpt* R package, which compares constant, trend, and AR(1) models with and without changepoints within a unified likelihood framework using Bayesian information criterion ranking (Killick *et al.,* 2018).

Exposure time series contained small filtered gaps (<20% missing values) which were imputed using Kalman smoothing with *na_kalman* from the *imputeTS* package (Moritz and Bartz-Beielstein, 2017). Because conventional cross-correlation can produce spurious lag structure under non-stationary conditions (Cheng *et al.,* 2021), lag dependence was examined using cross-entropy (Giannerini and Goracci, 2023a). Cross-entropy quantifies lagged dependence by measuring the divergence between the joint distribution $f_{X_t,Y_{t+k}}(x,y)$ and marginal distribution $f_{X_t}(x)f_{Y_{t+k}}(y)$. The statistic estimates the Hellinger-type distance between these distributions, which equals zero under independence and increases with nonlinear dependence, in practice the reference bandwidth and summation methods were used along with 500 bootstrap checks for p-values estimates (Giannerini and Goracci, 2023b).

Cross wavelet coherence was also computed using the Morlet mother wavelet in the R package *biwavelet* (Gouhier *et al.,* 2012), with significance tested against an AR1 red-noise background via 1,000 Monte Carlo surrogates; only regions within the cone of influence and exceeding the 95 % threshold were interpreted. Interpretation focused on coherent regions (black contours) with upwards arrows, reflecting phytoplankton-leading variability in marine aerosol. Arrows pointing right correspond to in-phase behaviour (concurrent increase) and left to anti-phase (i.e. phytoplankton lysis while marine aerosol increase). Coherence patches exhibiting rapidly rotating or opposing phase arrows within the same significant region were not interpreted, as illustrated in **Figure S4**, which shows unstable phase relationships between PMOA and eBC. The same pairwise comparison also fails the cross-entropy test, exhibiting no statistically robust lag structure, confirming that the apparent association is spurious rather than directional.

https://doi.org/10.5194/egusphere-2026-2745
Preprint. Discussion started: 27 May 2026

3. Results and Discussions

3.1 Temporal Dynamics and Biogeographic Patterns of Phytoplankton Functional Types

Daily biomass fields for major PFTs are first assessed against known established ecological seasonal and regional patterns to ensure model qualitative consistency with literature. **Figure S5** shows the North Atlantic weighted averages time series of seasonal dynamics of PFT biomass over a full year (2018) overlaid with changepoint analysis structural breaks. The weighted average is made from every grid cell retrieval from region bounded by 20°-66°N and 72°W-0° longitude (**Figure S6**), similar to Mansour *et al.* (2024).

Changepoint analysis shows a temporally ordered succession consistent with canonical bloom dynamics as diatoms enter the spring-summer climax phase on March 16th , followed by dinoflagellates on April 6th , haptophytes on April 17th , and chlorophytes on April 30th , consistently with typical PFT succession (Needham and Fuhrman, 2016). The diatoms climax phase persists until July 17th , after which their relative biomass declines steadily as diatoms are expected to progress into the stratified nutrients-limited depletion phase (Behrenfeld *et al.,* 2019). Further autumn to winter restructuring is also observed with *Prochlorococcus* and other prokaryotes increasing on September 22nd, and subsequent prokaryotic reorganisations on December 6th and 20th as the winter transition to deep mixing conditions sets in (Behrenfeld *et al.,* 2019). This increase is also consistent with the well-known rise in prokaryotes following seasonal entrainment of thermocline material and deep-ocean taxa into surface waters (Wenley *et al.,* 2021) whereas their strongly fluctuating standard deviation reflects patchy mesoscale filaments and eddy structures typical of prokaryotic mesoscale filaments (Gray *et al.,* 2024).

To further explore spatial variability in surface concentrations, AIGD-PFT data are split into bioregions following Longhurst biomes delineation (Longhurst, 2010) (**Figure 1)** with respective contributions (%) to PFT chl-*a* biomass shown in **Table S1**. Overall, throughout the year and all Longhurst provinces, diatoms biomass is prevailing (19.4%-65.5%), only closely followed by chlorophytes (15.7%-32.3%), haptophytes (4.7%-23.7%) and cryptophytes (5.2%-8.7%). Dinoflagellates remain relatively constant across basins (~5%), consistently with the ~5% relative abundance reported in previous field studies in the Western North Atlantic (Wang *et al.,* 2021) and in the subtropical North Atlantic (Duhamel *et al.,* 2019a). In contrast to this, *Prochlorococcus* (0.9-7.6%) and other prokaryotes (0.6-6.7%) display a clear south-north concentrations gradient, with higher contributions at lower latitudes (consistent with observations of increasing cyanobacterial dominance toward subtropical regions; Bolaños *et al.,* 2021) whereas pelagophytes remain minor (0.9-3.1%). In addition, haptophytes visibly decline in the boreal polar region (4.7%), where diatoms are known to outcompete them (Krisch *et al.,* 2020; Pierella Karlusich *et al.,* 2025). Overall, the relative ordering of total surface phytoplankton biomass across Longhurst provinces is consistent with *in-situ* Atlantic transect observations, with lowest biomass in oligotrophic gyres and enhanced biomass in subpolar and shelf regions (Brotas *et al.,* 2022).

https://doi.org/10.5194/egusphere-2026-2745
Preprint. Discussion started: 27 May 2026

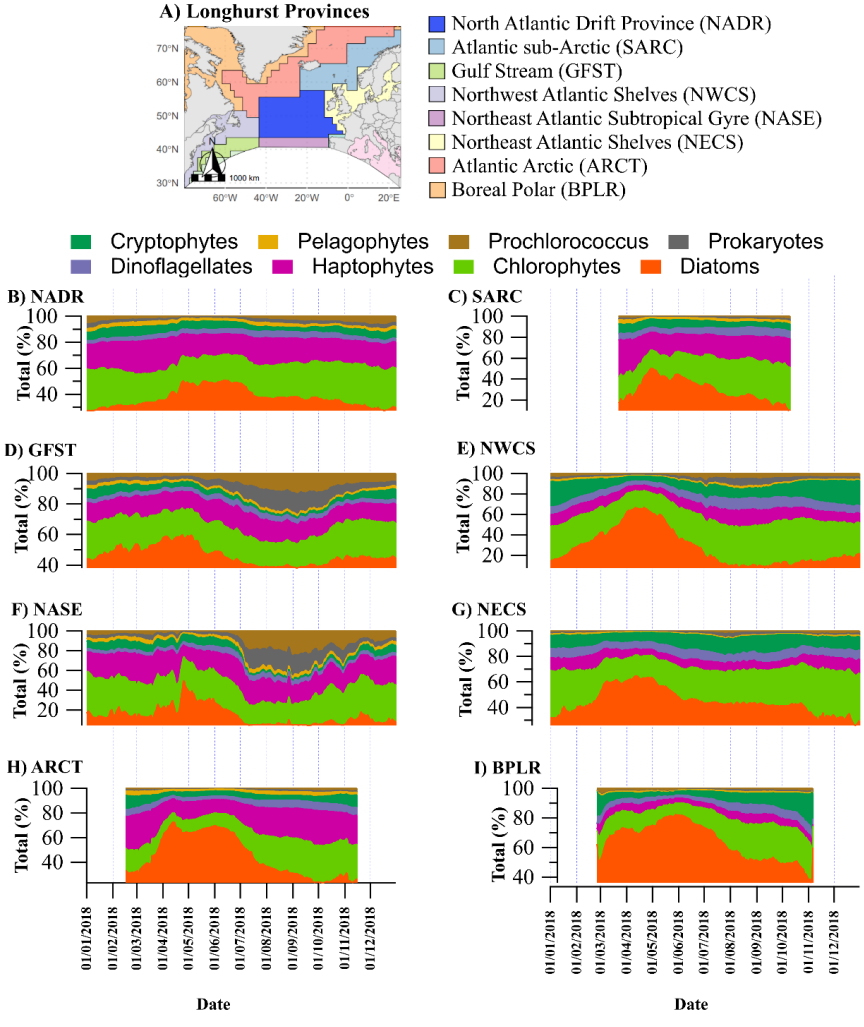

Figure 1. Weighted averages of Phytoplankton functional types by Longhurst regions. BPLR: Boreal Polar, NADR: North Atlantic Drift, GFST: Gulf Stream, ARCT: Atlantic Arctic, SARC: Atlantic Subarctic, NASW: Northwest Atlantic subtropical gyre, NASE: Northeast Atlantic subtropical gyre, NECS: Northeast Atlantic shelf, NWCS: Northwest Atlantic shelf.

https://doi.org/10.5194/egusphere-2026-2745
Preprint. Discussion started: 27 May 2026

3.2 Primary marine organic aerosol constraining

To robustly estimate PMOA time series, PMOA was constrained using its characteristic mass spectral fingerprint previously established at Mace Head (Ovadnevaite *et al.,* 2011a) and shown in **Figure S7**. PMOA mass spectra comprise oxygenated carbons (CHO-type fragments) that dominate the mass spectra intensity (55%), followed by aliphatic fragments (C_xH_y) contributing 39%. Representative ion series include C_xH_{2y-3} (i.e. *m/z* 39.02, 53.03, 67.05, 81) for alkynes, dienes and cycloalkenes, $C_xH_{2y-1}CO$ (i.e. *m/z* 55.02, 69.03, 83.05) related to alkenyl groups, diunsaturates, cyclic alcohols, and ethers as well as C_xH_{2y+1} (i.e. *m/z* 15.02, 29.03, 37.00) reflecting alkyls fragments. Further descriptions and implications of PMOA fingerprint are provided in earlier Mace Head studies (Chevassus *et al.,* 2025; Ovadnevaite *et al.,* 2011b). For low factor solutions (3-5 factors; **Figure S7**), the retrieved PMOA time series across all *a*-values show unrealistic behaviour, with large spikes and artificial co-variability with eBC (R=0.35-0.62, **Figure S8**). Also, the six-factor solution provides a physically consistent representation, minimising correlation with eBC (R = 0.16**, Figure S9**). Seven or eight-factor solutions were not retained, as they showed the same PMOA correlations with external tracers than six factors, and furthermore, recent work also indicates that Mace Head submicron aerosols are best represented by six factors (Moschos *et al.,* 2026). Bootstrap diagnostics further support the selection of the six-factor solution (**Figure S10**). The reconstructed PMOA time series is stable across resamples, with uncertainty remaining small relative to peak amplitudes (**Figure S10A**). The Q/Qexp ratio decreases from 1.24 ± 0.02 (3 factors) to 1.03 ± 0.02 (4 factors), 0.88 ± 0.02 (5 factors), and 0.71 ± 0.02 for the six-factor solution (**Figure S10B**). The relative Q/Qexp variability stabilises beyond five factors (**Figure S10C**), and the incremental improvement in Q/Qexp becomes marginal after seven factors (**Figure S10D**). Residuals for the six-factor solution remain randomly distributed without systematic structure (**Figure S10E**) and finally, the bootstrap-derived uncertainty distribution is moderately skewed but well constrained (**Figure S10F**). The PMOA series from six-factor solution is presented in **Figure 2** as a dashed blue line. PMOA concentrations peaked in late spring-early summer, with a sharp maximum in early July, reflecting the PFT bloom climax, concentrations then declined through late summer (August) and remained low during autumn-winter with only minor fluctuations (**Figure S10**). Two contrasting cases were then retained: The Northeast Atlantic shelves (NECS) during phytoplankton bloom climax (May 25th to July 13th 2018) and the North Atlantic drift province (NADR) during late summer early depletion (Both August 2018 and August 2009, with the latter featuring PMOA concentrations one order of magnitude higher than August 2018)

3.3 Exposure to phytoplankton functional types, micronekton and aerosol seasonal source regions

Since AIGD-PFT can capture real world phytoplankton growth dynamics, with coherent ecological succession across space and time, the atmospheric consequences of these dynamics are examined next. During the spring-summer climax bloom, PMOA closely tracks recent biological activity (**Figure 2A,**

https://doi.org/10.5194/egusphere-2026-2745
Preprint. Discussion started: 27 May 2026

315 **S9**), with strong correlations for dinoflagellates (R = 0.70), cryptophytes (R = 0.68), diatoms (R = 0.65), and chlorophytes (R = 0.62). Conversely, haptophytes (R = 0.30), prokaryotes (R = 0.32), and pelagophytes (R = 0.21) exhibit weaker values, while *Prochlorococcus* shows no measurable relationship (R = -0.02).

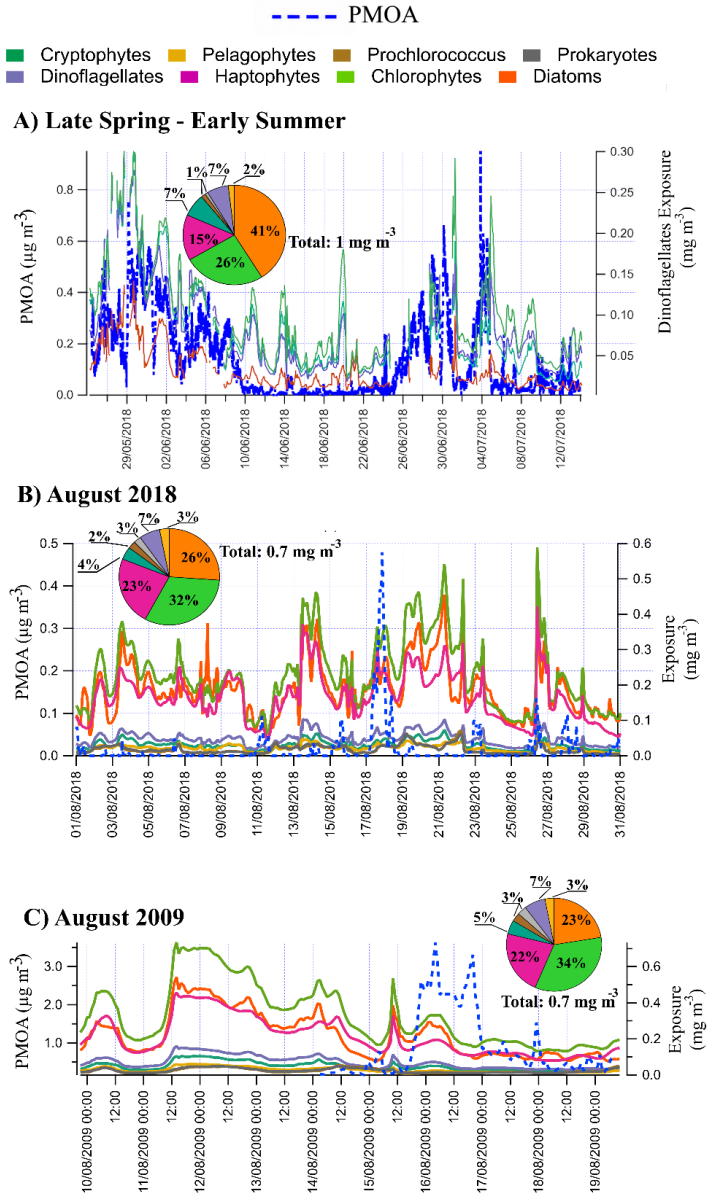

https://doi.org/10.5194/egusphere-2026-2745
Preprint. Discussion started: 27 May 2026

Figure 2. Primary marine organic aerosol (PMOA) time series and associated phytoplankton functional type (PFT) air masses exposure for A) Climax phase - May 25th to July 13th 2018), B) Depletion phase - August 2018, and C) August 2009. PMOA concentrations (left y-axis; dashed blue lines) are shown together with the cumulative PFT exposure along the 72-h back trajectories (right y-axis). Insets report the relative PFT composition (percentage contribution and total exposure) for each period.

Furthermore, these PFT correlation values are partly in line with PMOA-related measurements literature correlation values (**Table S2**) although values are highly specific to sampling location and are generally lacking for the North Atlantic. For instance, the HR-ToF-AMS correlations with the main PFT obtained here (R = 0.60-0.70) are comparable to those reported for sea spray fluorescence (SSF) and chlorophytes in the Southern Ocean (Moallemi *et al.,* 2021), similar to those found for haptophytes in the Mediterranean (Sellegri *et al.,* 2021) but lower than the strong correlations with diatoms observed in the Amundsen Sea (Jung *et al.,* 2020). Conversely, diatoms and dinoflagellates relationships fall within the same range as CCN-based correlations (Schwier *et al.,* 2017) reported for the Mediterranean (R ≈ 0.60), except for *Prochlorococcus* (Schwier *et al.,* 2015) which shows negligible association here while the link with cryptophytes is substantially stronger in this study than the weak or absent relationships found between PMOA and cryptophytes in the Mediterranean (Freney *et al.,* 2020; Trueblood *et al.,* 2021). In contrast to this spring-summer climax, the early depletion phase North Atlantic open-ocean (NADR) PMOA source in August 2018 (**Figure 2B**) or August 2009 (**Figure 2C**) are characterised by PFT spikes preceding PMOA variability which weakens the apparent contemporaneous correlations (**Figure S11**) and instead suggests a more lagged response, investigated in section 3.4 below.

In addition, air-masses exposure to micronekton concentrations (**Figure S12**) span 3.3 ± 2.1 gC m^{-2} (August 2018), 5.6 ± 2.3 gC m^{-2} (spring-summer 2018), and 11.2 ± 1.6 gC m^{-2} (August 2009), with PMOA-micronekton correlations (R ≈ 0.55, -0.20, and -0.11, respectively) following the same structure as PFT, with micronekton spikes also preceding PMOA (**Figure S13**). PMOA-micronekton variations align in a first-order sense with previous Arctic measurements reporting substantial enrichment of humic-like organic material in PMOA (40-280% relative to seawater) associated with delayed zooplankton grazing and excretion processes (Dall'Osto *et al.,* 2025). Micronekton concentrations were nearly 3 times higher in August 2009 (**Figure 2C**) than in August 2018 (**Figure S13**), coinciding with an almost one order of magnitude elevation in PMOA concentrations, although this also reflected more efficient air-sea transfer conditions as detailed below.

https://doi.org/10.5194/egusphere-2026-2745
Preprint. Discussion started: 27 May 2026

To further investigate potential drivers, PMOA source regions are identified using simplified quantitative transport bias analysis. Two dominant source regions are resolved: The North Atlantic Drift (NADR) region and the Northeast European Continental Shelf (NECS) region (**Figure 3**).

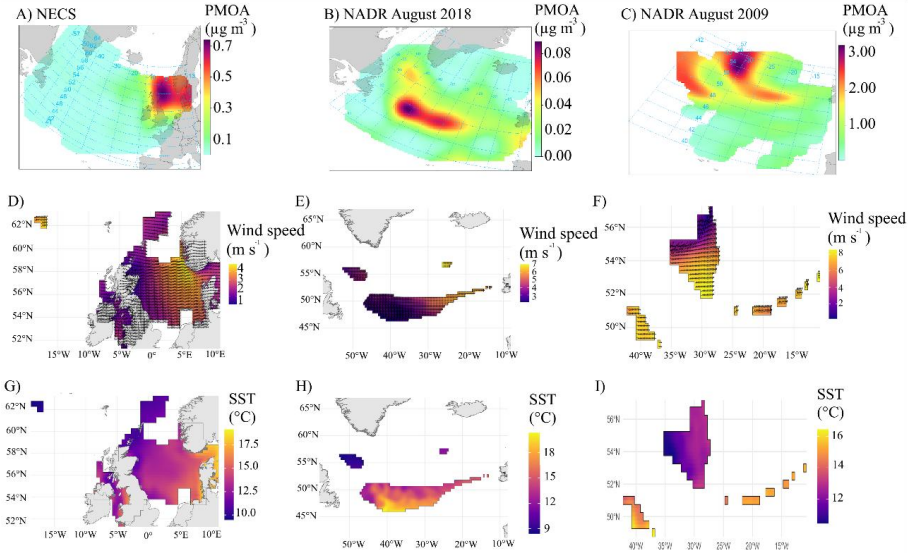

Figure 3. Simplified quantitative transport bias analysis (SQTBA) for primary marine organic aerosol during A) May 25th to July 13th 2018, B) August 2018, and C) August 2009. Panels D-F) show the corresponding 10-m wind speed fields from ERA5 for the same periods, and panels G-I) show the associated sea-surface temperatures (SST). Each map displays only the grid cells contributing to the top 10 % of the PMOA back-trajectory mass concentrations footprint for each event.

Wind speed explains the enhanced PMOA concentrations observed in August 2009. Winds during May-July 2018 (climax phase) were weak (median 1.66 m s^{-1}; inter quartile: 0.57-3.77 m s^{-1}), increasing in August 2018 (median 3.45 m s^{-1}; 2.48-6.00 m s^{-1}), but still not reaching substantially higher values that were observed in August 2009 (median 6.83 m s^{-1}; 2.40-8.13 m s^{-1}). These stronger winds in August 2009 sustained wave breaking and bubble plume formation, promoting shallow bubble-layer renewal and deeper plume penetration, thereby increasing the probability that bubbles resurface and burst (Czerski *et al.,* 2022). At the same time, winds >4-6 m s^{-1} also disrupt bacterioneuston (Rahlff *et al.,* 2017), mixing surface organics and bacteria into the upper water column where they become more readily accessible to bubbles. This progression in wind forcing was accompanied by a coherent shift in wave-state parameters (**Figure S14**). Significant wave height increased from 1.14 m (0.50-1.72 m) in spring-summer 2018, to 1.76 m (1.60-2.06 m) in August 2018, and 2.50 m (2.17-2.73 m) in August 2009, while the wave Reynolds number rose from 1.86 × 10^5 (7.41 × 10^4-2.96 × 10^5) to 3.24 × 10^5 (2.76 × 10^5-4.63 × 10^5) and 5.88 × 10^5 (4.18 × 10^5-7.47 × 10^5).

https://doi.org/10.5194/egusphere-2026-2745
Preprint. Discussion started: 27 May 2026

The Reynolds number integrates wind stress, wave height, and water viscosity and therefore directly reflects more efficient bubble-mediated aerosol production (Ovadnevaite *et al.,* 2014a) as can be seen in August 2009 here.

Atmospheric stability also strengthened from 0.18 °C (-0.65-0.48 °C) in spring-summer 2018 to 0.21 °C (-0.28-0.85 °C) in August 2018 and 0.49 °C (0.05-1.18 °C) in August 2009, implying a shift toward conditions where whitecaps could be sustained (Markuszewski *et al.,* 2024), while SST ranged from 10.9-15.7 °C (median 13.3 °C) in spring-summer 2018, 9.6-17.8 °C (14.9 °C) in August 2018, and 10.4-16.1 °C (12.6 °C) in August 2009. These values sit well above the <8 °C regime in which Sellegri *et al.,* (2023) observed a strong, four-fold enhancement of sea spray flux. Yet, the 1.7-5.3 °C cooling in August 2009 relative to 2018 led to increased viscosity (**Figure S14**), which is known to slow down microbial degradation rates (Guadayol *et al.,* 2021), leading to stabilised gel-like particles and colloids, all of which can increase the persistence of surface-active material available for bubble scavenging at the sea-air interface as cooler, thicker, bubble films are formed (Hu *et al.,* 2024). In addition, colder SST systematically increase the degree of lipid unsaturation in planktonic membranes as part of a homeoviscous adaptation that preserves membrane fluidity and enzymatic activity (Holm *et al.,* 2022; Liu *et al.,* 2025a) which in principle increases the pool of surface-active organic precursors available for bubble scavenging. Similarly, cooler conditions are also known to favour viral production and viral lysis efficiency thereby further concurring to PMOA formation (Anesio and Bellas, 2011; Demory *et al.,* 2021). Taken together, the contrasting wind, waves, and temperatures help clarify why PMOA amplitudes differ across periods with similar phytoplankton exposure and hint at PMOA plumes spiking after PFT increase with more or less delay, as such, temporally resolved approaches (Ali *et al.,* 2024) are next explored to disentangle genuine source-receptor dynamics.

3.4 Lag estimates and synergistic-unique-redundant decomposition

For primary marine organic aerosol (PMOA) during the spring-summer climax phase, PMOA-PFT cross entropy shows significant lags between PMOA and several PFT. Significant lags are observed for cryptophytes from 2 to 25 days, dinoflagellates from 2 to 28 days, diatoms from 2 to 25 days, and chlorophytes from 3 to 25 days. Longer-lag contributions are detected for haptophytes at 25 days, *Prochlorococcus* at 15 and 28 days, and other prokaryotes at 25 days while pelagophytes show no significant lagged association with PMOA (**Figure 4**). Overall, cross-entropy scores from haptophytes, *Prochlorococcus* and other prokaryotes were half those of cryptophytes, diatoms, dinoflagellates and chlorophytes that form a clear upper tier. This might be explained by *Prochlorococcus* and other prokaryotes being comparatively less intense lipid emitters (Becker *et al.,* 2025) whereas pelagophyte biomass is extremely small over the North Atlantic (2.7%). In addition, diatoms, dinoflagellates, cryptophytes and chlorophytes all have similar PMOA lag patterns, with a first early-bloom-stage (~2-3 days) followed by a lysis-stage after 25 days (also seen in haptophytes and prokaryotes), hinting at both lysis and/or late stage prokaryote-diatoms interactions sustaining exopolymers production

https://doi.org/10.5194/egusphere-2026-2745
Preprint. Discussion started: 27 May 2026

(Zamanillo *et al.,* 2019). Furthermore, micronekton ranks alongside the upper-tier PFTs with peaks at 2 days and additional contributions near 10 and 30 days, indicating that trophic-level processes contribute to PMOA at magnitudes comparable to direct phytoplankton emissions, plausibly through bubble-mediated enrichment of lipid-rich faecal pellets and excretion products.

For MSA, cross entropy during the same climax phase further shows a significant maximum information transfer between MSA and cryptophytes at lags of 4 and 9 days, dinoflagellates at 5 days and 9 days, diatoms at 9 days, chlorophytes at 4 and 9 days, haptophytes, pelagophytes, *Prochlorococcus* at 30 days and other prokaryotes at 4 days. These lags span over nascent blooms (~4 days) to intermediate lags (~9 days) hinting at delayed bloom senescence, and a long lag (~30 days) phase specifically showing for *Prochlorococcus*. This long lag likely reflects *Prochlorococcus* having limited DMSP-cleaving enzyme activity, shifting late-stage DMS production to bacteria, viruses, or enzymes species decoupled from the initial bloom phase (Malfatti *et al.,* 2019).

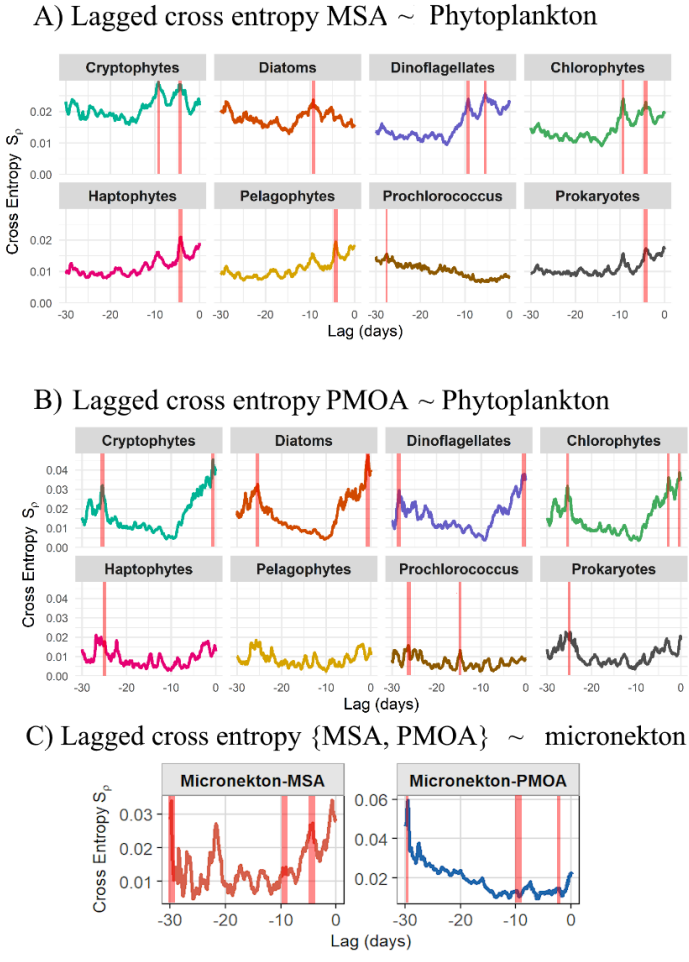

https://doi.org/10.5194/egusphere-2026-2745
Preprint. Discussion started: 27 May 2026

Figure 4. Lagged cross-entropy during the spring-summer climax between A) PMOA and PFT, B) Lagged cross-entropy between MSA and PFT, C) Lagged cross-entropy between PMOA, MSA and micronekton. Significant lags obtained with bootstrapping are highlighted with a small red star (n = 1189, 1 h resolution).

Micronekton cross-entropy with MSA also peaks at 4 days with secondary contributions near 10 and 30 days which is consistent with grazing-driven DMS release followed by atmospheric oxidation, though it does not exclude behavioural aggregation of higher trophic levels along DMS gradients acting as chemosensory cues (Owen *et al.,* 2021) or substantial DMS release from planktivory micronekton or lower-trophic level grazing (e.g. copepods grazing on dinoflagellates; Dacey and Wakeham, 1986). Overall, the PFT-micronekton contributions ranking for MSA is markedly diffuse as MSA is the product of a multi-step pathway (DMSP → DMS → multi-oxidant atmospheric chemistry) where atmospheric oxidation results in homogenised source-specific signatures.

More subtle and transient lagged coupling patterns were also investigated to explain the differences between the spring-summer climax phase and the august depletion phase from April to August 2018 using bivariate wavelet analysis. This metric quantifies the local correlation between two non-stationary signals as a function of time and period, with values approaching 1 denoting strong co-variability. In **Figure S15**, arrows pointing right correspond to in-phase behaviour, left to anti-phase (i.e. phytoplankton lysis concurrent with increases in PMOA), upward to phytoplankton leading PMOA, and downward to PMOA leading phytoplankton. Coherence between PMOA and diatoms, dinoflagellates, haptophytes and cryptophytes is largely confined to spring and early summer, with no significant coupling for these species persisting into August. Conversely, chlorophytes, *Prochlorococcus* and other prokaryotes displayed a distinct 9-11 day period coherence patch, significant against an AR(1) red-noise background (black contour), with anti-phase orientation (arrows pointing left) typical of phytoplankton lysis concomitant with lagged PMOA increase. This phase coherence points towards a (weaker) persistence of the phytoplankton-PMOA senescent coupling even during the depletion phase. In other words, PMOA sources shift away from diatoms, dinoflagellates, haptophytes and cryptophytes during the spring-summer climax to only chlorophytes, *Pro*chl*orococcus* and other prokaryotes during the late summer depletion stage.

Finally, raw chl-*a* time series exhibited weaker correlations with PMOA (R = 0.43 and 0.28) than PFTs but improved substantially after Hampel outliers filtering (R = 0.59 and 0.60) while still showing weakly significant paired cross-entropy at 2-4 days and missing out on longer lysis related lags (**Figure S16**). This likely reflects the confounding influence of optical and biogeochemical artefacts, such as photoacclimation, lysis by-products (phaeophytin, chlorophyllide), and radiative interferences from post-bloom organic matter (Prochaska and Frouin, 2024; Simis *et al.,* 2007), which obscure true biomass signals. In oligotrophic regions, chl-*a* increases may even arise from light-driven physiological adjustments rather than nutrient-fueled growth (Liu *et al.,* 2025b). While lag-adjusted chl-*a* generally correlates moderately well with sea spray organics (O'Dowd *et al.,* 2015), its

https://doi.org/10.5194/egusphere-2026-2745
Preprint. Discussion started: 27 May 2026

reliability as a productivity proxy is known to degrade over senescent blooms or oligotrophic waters (Collins *et al.,* 2016). PFTs and micronekton, however, manage to capture more plausible early bloom emissions and late-stage lysis lags. This advantage is rooted in AIGD-PFT's combination of input pigment data (for which degradation products are carefully treated; Roesler *et al.*, 2017; Swan *et al.*, 2016) and multi-source environmental inputs which allow here for ecologically coherent marine organic aerosol lag resolution (Zhang *et al.,* 2024).

4. Conclusion

By combining a full year of high-resolution aerosol mass spectrometry at Mace Head with HYSPLIT-derived air-mass exposure to gap-free phytoplankton functional type (PFT) and micronekton fields, this study delivers four main contributions to the understanding of marine organic aerosols.

First, the PMOA-PFT connections shift throughout the year, from diatoms, dinoflagellates, haptophytes and cryptophytes during the spring-summer climax, to only chlorophytes, *Prochlorococcus* and other prokaryotes during the late summer depletion stage. During the spring-summer climax, diatoms, dinoflagellates, chlorophytes, and cryptophytes all covaried along with PMOA. This is expected since diatoms are the main PFT biomass contributors as well as one of the main producers of organic carbon (Hansell *et al.,* 2024; Lu *et al.,* 2025), cryptophytes have significant lipids content (Taipale *et al.,* 2020), chlorophytes are abundant in the North-East Atlantic and known to be strong aliphatic and alcohol emitters (Duhamel *et al.,* 2019b) whereas dinoflagellates are also known to be active emitters of various fatty acids (Bi *et al.,* 2019). Conversely, haptophytes are less significant despite their ability to also emit aliphatic and alcohol during viral lysis or open ocean oligotrophic starvation (Fulton *et al.,* 2014; Malitsky *et al.,* 2016; Rosenwasser *et al.,* 2014). Nevertheless, this taxonomic framing remains context-dependent, as plankton lipidomes broadly vary across regions and species assemblages (Liu *et al.,* 2025a)

Second, MSA showed a broader and less taxonomically concentrated PFT signature than PMOA. While several diatom taxa are known to exceed haptophytes in cellular DMSP (Bullock *et al.,* 2017; Shemi *et al.,* 2023) and despite their overwhelming biomass in polar and subarctic blooms where they tend to dominate system-level DMSP production and associated sulphur emissions (Dani and Loreto, 2017; Jang *et al.,* 2019), no such prevalence can be ascertained here. Conversely, haptophytes and pelagophytes distinctively contributed as early-stage DMS sources, whereas *Pro*chl*orococcus* were rather associated with a delayed lysis-stage. Overall, these results are consistent with recent DMS literature reporting that diatoms, cryptophytes and chlorophytes once thought to lack DMSP lipase enzyme, may in fact all be new emerging players in the marine sulphur cycle (Shemi et al., 2023; Wang et al., 2024).

Third, this study provides observational evidence that higher trophic levels contribute directly to PMOA with cross-entropy placing micronekton contributions alongside the upper-tier PFTs. While the

https://doi.org/10.5194/egusphere-2026-2745
Preprint. Discussion started: 27 May 2026

contribution of micronekton (or that of zooplankton; Dall'Osto *et al.*, 2025) to epipelagic organic carbon is well established, with pellets and dead bodies accounting for a substantial fraction of their total carbon production (Thibault *et al.,* 2025), their contributions to marine organic aerosols are still globally underexplored.

Fourth, the phytoplankton-aerosol coupling was found to be modulated by both ecosystem succession and air-sea physics. The spring-summer 2018 shelf climax, under calm winds and moderate wave breaking, rapidly produced PMOA whereas August 2018, despite comparable phytoplankton exposure, gave a weak and more lagged PMOA response, as warmer SST and low wave Reynolds numbers limited bubble plume penetration and film drops. August 2009 instead produced a strong but lagged PMOA response: cooler SST raised viscosity and stabilised gel-like surfactants, higher significant wave heights and a markedly larger wave Reynolds number sustained breaking waves and film drops so the same PFT pool was transferred to the atmosphere far more efficiently.

Several mechanisms may also account for the temporal and spatial variability observed in phytoplankton-aerosol coupling. First, changes in the concentration and composition of surface-active compounds can alter bubble film thickness and lifetime, thereby modulating the organic enrichment of sea spray aerosol (Ovadnevaite et al., 2017; Sellegri et al., 2021). Second, seasonal shifts in microbial processing may influence the availability of organic precursors, with enhanced microbial recycling during summer compared to spring and spatial variability in viral lysis rates across oceanic regions (Eigemann *et al.,* 2024; Mojica *et al.,* 2016). Third, not all biological activity is represented (e.g. viruses, archaea, fungi), nor is the significant functional diversity within taxa or synergistic effects. Fourth, switches to mixo-/heterotrophy over time within groups as well as differences in PFT cells sizes can in principle strongly change marine organic aerosols emission. Fifth, microbial communities can eventually transition to act as a net DMS sink rather than source (Le Gland *et al.,* 2024). Lastly, recent evidence suggests that temperature effects also propagate through delayed biological responses in productivity with thermal history shaping phytoplankton performance (Anderson *et al.,* 2025) and community-level responses being modulated by a sequences of prior warm and cool phases (Wolf *et al.,* 2024).

In conclusion, these results motivate future research vessel campaigns and mesocosm experiments to explicitly manipulate PFT interactions and air-sea physics. Such experiments still remain scarce, often focusing on single species (i.e. pseudo-axenic cultures) such as the coccolithophore *Emiliania huxleyi* (O'Dowd *et al.,* 2015) or diatoms like *Thalassiosira pseudonana* or *Nitzchia closterium* (Alpert *et al.,* 2015; Sellegri *et al.,* 2021). Accordingly, mesocosm studies have yet to completely capture the role of fully resolved PFT assemblages and neuston interactome (Martínez-Pérez et al., 2024) in marine organic aerosols formation, and to explicitly resolve non-linear temperature-biology interactions and realistic wave breaking conditions (Anderson *et al.,* 2025; Liu *et al.,* 2024; Sellegri *et al.,* 2024)

https://doi.org/10.5194/egusphere-2026-2745
Preprint. Discussion started: 27 May 2026

Author contributions. JO, CO'D, and DC designed the research. DC, JO, VM and KNF operated the instruments and verified the raw data processing. EC, VM and JO produced the postprocessed data and figures. JO, CO'D, DC, WX, LC, VM, DS, LL and VP reedited the manuscript. EC wrote the paper with support from all authors, who commented on the paper.

Competing interests. The authors declare that they have no conflict of interest.

Acknowledgments. This work was supported by Taighde Éireann - Research Ireland under Grant number 22/FFP-A/10611, the Department of the Environment, Climate and Communications, the Environmental Protection Agency (EPA) of Ireland (AC3 network) and the University of Galway College of Science and Engineering Postgraduate Fellowship n°127407.

Data availability. The codes supporting the analyses presented in this study will be made openly available on https://zenodo.org/records/20155093. The observational time series from the Mace Head Atmospheric Research Station are available from the corresponding author upon request, with a later release planned on EBAS. Phytoplankton functional type fields are available from the AIGD-PFT dataset (https://doi.org/10.5194/essd-16-4793-2024) while global 9 km gap-filled chl-*a* and suspended particulate matter (SPM) were retrieved from ftp://ftp.star.nesdis.noaa.gov/pub/socd1/mecb/coastwatch/viirs/science/L3/global. Micronekton and zooplankton can be accessed online from the Copernicus Marine Service GLOBAL_MULTIYEAR_BGC_001_033 dataset (https://doi.org/10.48670/moi-00020), while meteorological data are available from ERA5 services (https://doi.org/10.24381/cds.adbb2d47).

References

Albernhe, S., Gorgues, T., Lehodey, P., Menkes, C., Titaud, O., Magon De La Giclais, S., and Conchon, A.: Global characterization of modelled micronekton in biophysically defined provinces, Progress in Oceanography, 229, 103370, https://doi.org/10.1016/j.pocean.2024.103370, 2024.

Ali, S., Hasan, U., Li, X., Faruque, O., Sampath, A., Huang, Y., Gani, M. O., and Wang, J.: Causality for Earth Science -- A Review on Time-series and Spatiotemporal Causality Methods, https://doi.org/10.48550/ARXIV.2404.05746, 2024.

Alpert, P. A., Kilthau, W. P., Bothe, D. W., Radway, J. C., Aller, J. Y., and Knopf, D. A.: The influence of marine microbial activities on aerosol production: A laboratory mesocosm study, JGR Atmospheres, 120, 8841–8860, https://doi.org/10.1002/2015JD023469, 2015.

Alsante, A. N., Thornton, D. C. O., Brooks, S. D., Mirrielees, J. A., Wilbourn, E. K., Matthews, B. H., Diaz, B. P., and Bidle, K. D.: Effect of viral infection on the ice nucleation efficiency of marine coccolithophores, Aerosol Science and Technology, 59, 195–213, https://doi.org/10.1080/02786826.2024.2420675, 2025.

https://doi.org/10.5194/egusphere-2026-2745
Preprint. Discussion started: 27 May 2026

Anderson, D. M., Fey, S. B., Meier, H. S., Vasseur, D. A., and Kremer, C. T.: Nutrient storage links past thermal exposure to current performance in phytoplankton, Proc. Natl. Acad. Sci. U.S.A., 122, e2418108122, https://doi.org/10.1073/pnas.2418108122, 2025.

Anesio, A. M. and Bellas, C. M.: Are low temperature habitats hot spots of microbial evolution driven by viruses?, Trends in Microbiology, 19, 52–57, https://doi.org/10.1016/j.tim.2010.11.002, 2011.

Bar-On, Y. M. and Milo, R.: The Biomass Composition of the Oceans: A Blueprint of Our Blue Planet, Cell, 179, 1451–1454, https://doi.org/10.1016/j.cell.2019.11.018, 2019.

Beaupré, S. R., Kieber, D. J., Keene, W. C., Long, M. S., Maben, J. R., Lu, X., Zhu, Y., Frossard, A. A., Kinsey, J. D., Duplessis, P., Chang, R. Y.-W., and Bisgrove, J.: Oceanic efflux of ancient marine dissolved organic carbon in primary marine aerosol, Sci. Adv., 5, eaax6535, https://doi.org/10.1126/sciadv.aax6535, 2019.

Becker, K. W., Devresse, Q., Prieto-Mollar, X., Hinrichs, K.-U., and Engel, A.: Mixed-layer lipidomes suggest offshore transport of energy-rich and essential lipids by cyclonic eddies, Commun Earth Environ, 6, 179, https://doi.org/10.1038/s43247-025-02152-0, 2025.

Behrenfeld, M. J., Moore, R. H., Hostetler, C. A., Graff, J., Gaube, P., Russell, L. M., Chen, G., Doney, S. C., Giovannoni, S., Liu, H., Proctor, C., Bolaños, L. M., Baetge, N., Davie-Martin, C., Westberry, T. K., Bates, T. S., Bell, T. G., Bidle, K. D., Boss, E. S., Brooks, S. D., Cairns, B., Carlson, C., Halsey, K., Harvey, E. L., Hu, C., Karp-Boss, L., Kleb, M., Menden-Deuer, S., Morison, F., Quinn, P. K., Scarino, A. J., Anderson, B., Chowdhary, J., Crosbie, E., Ferrare, R., Hair, J. W., Hu, Y., Janz, S., Redemann, J., Saltzman, E., Shook, M., Siegel, D. A., Wisthaler, A., Martin, M. Y., and Ziemba, L.: The North Atlantic Aerosol and Marine Ecosystem Study (NAAMES): Science Motive and Mission Overview, Front. Mar. Sci., 6, 122, https://doi.org/10.3389/fmars.2019.00122, 2019.

Bi, Y., Wang, F., and Zhang, W.: Omics Analysis for Dinoflagellates Biology Research, Microorganisms, 7, 288, https://doi.org/10.3390/microorganisms7090288, 2019.

Bolaños, L. M., Choi, C. J., Worden, A. Z., Baetge, N., Carlson, C. A., and Giovannoni, S.: Seasonality of the Microbial Community Composition in the North Atlantic, Front. Mar. Sci., 8, 624164, https://doi.org/10.3389/fmars.2021.624164, 2021.

Brockmann, J. E.: Aerosol Transport in Sampling Lines and Inlets, in: Aerosol Measurement, edited by: Kulkarni, P., Baron, P. A., and Willeke, K., Wiley, 68–105, https://doi.org/10.1002/9781118001684.ch6, 2011.

https://doi.org/10.5194/egusphere-2026-2745
Preprint. Discussion started: 27 May 2026

Brotas, V., Tarran, G. A., Veloso, V., Brewin, R. J. W., Woodward, E. M. S., Airs, R., Beltran, C., Ferreira, A., and Groom, S. B.: Complementary Approaches to Assess Phytoplankton Groups and Size Classes on a Long Transect in the Atlantic Ocean, Front. Mar. Sci., 8, 682621, https://doi.org/10.3389/fmars.2021.682621, 2022.

Bullock, H. A., Luo, H., and Whitman, W. B.: Evolution of Dimethylsulfoniopropionate Metabolism in Marine Phytoplankton and Bacteria, Front. Microbiol., 8, https://doi.org/10.3389/fmicb.2017.00637, 2017.

Burrows, S. M., Easter, R. C., Liu, X., Ma, P.-L., Wang, H., Elliott, S. M., Singh, B., Zhang, K., and Rasch, P. J.: OCEANFILMS (Organic Compounds from Ecosystems to Aerosols: Natural Films and Interfaces via Langmuir Molecular Surfactants) sea spray organic aerosol emissions – implementation in a global climate model and impacts on clouds, Atmos. Chem. Phys., 22, 5223–5251, https://doi.org/10.5194/acp-22-5223-2022, 2022.

C. Corbin, J., Othman, A., D. Haskins, J., D. Allan, J., Sierau, B., R. Worsnop, D., Lohmann, U., and A. Mensah, A.: Peak fitting and integration uncertainties for the Aerodyne Aerosol Mass Spectrometer, Aerosols/In Situ Measurement/Instruments and Platforms, https://doi.org/10.5194/amtd-8-3471-2015, 2015.

C3S: ERA5 hourly data on single levels from 1940 to present, https://doi.org/10.24381/CDS.ADBB2D47, 2018.

Cala, B. A., Archer-Nicholls, S., Weber, J., Abraham, N. L., Griffiths, P. T., Jacob, L., Shin, Y. M., Revell, L. E., Woodhouse, M., and Archibald, A. T.: Development, intercomparison and evaluation of an improved mechanism for the oxidation of dimethyl sulfide in the UKCA model, Gases/Atmospheric Modelling/Troposphere/Chemistry (chemical composition and reactions), https://doi.org/10.5194/acp-2023-42, 2023.

Campbell, J. W.: The lognormal distribution as a model for bio-optical variability in the sea, J. Geophys. Res., 100, 13237–13254, https://doi.org/10.1029/95JC00458, 1995.

Canonaco, F., Crippa, M., Slowik, J. G., Baltensperger, U., and Prévôt, A. S. H.: SoFi, an IGOR-based interface for the efficient use of the generalized multilinear engine (ME-2) for the source apportionment: ME-2 application to aerosol mass spectrometer data, Atmos. Meas. Tech., 6, 3649–3661, https://doi.org/10.5194/amt-6-3649-2013, 2013.

Chebaicheb, H. and Riffault, V.: User guide for ACSM data processing and PMF application using SoFi Pro, 2025.

https://doi.org/10.5194/egusphere-2026-2745
Preprint. Discussion started: 27 May 2026

Cheng, Y., Hui, Y., McAleer, M., and Wong, W.-K.: Spurious Relationships for Nearly Non-Stationary Series, JRFM, 14, 366, https://doi.org/10.3390/jrfm14080366, 2021.

Chevassus, E., Fossum, K. N., Ceburnis, D., Lei, L., Lin, C., Xu, W., O'Dowd, C., and Ovadnevaite, J.: Marine organic aerosol at Mace Head: effects from phytoplankton and source region variability, Atmos. Chem. Phys., 25, 4107–4129, https://doi.org/10.5194/acp-25-4107-2025, 2025.

Collins, D. B., Bertram, T. H., Sultana, C. M., Lee, C., Axson, J. L., and Prather, K. A.: Phytoplankton blooms weakly influence the cloud forming ability of sea spray aerosol: CCN From Algae Bloom Microcosms, Geophys. Res. Lett., 43, 9975–9983, https://doi.org/10.1002/2016GL069922, 2016.

Crespi, A., Bernardoni, V., Calzolai, G., Lucarelli, F., Nava, S., Valli, G., and Vecchi, R.: Implementing constrained multi-time approach with bootstrap analysis in ME-2: An application to PM2.5 data from Florence (Italy), Science of The Total Environment, 541, 502–511, https://doi.org/10.1016/j.scitotenv.2015.08.159, 2016.

Crocker, D. R., Hernandez, R. E., Huang, H. D., Pendergraft, M. A., Cao, R., Dai, J., Morris, C. K., Deane, G. B., Prather, K. A., and Thiemens, M. H.: Biological Influence on δ^{13}C and Organic Composition of Nascent Sea Spray Aerosol, ACS Earth Space Chem., 4, 1686–1699, https://doi.org/10.1021/acsearthspacechem.0c00072, 2020.

Czerski, H., Brooks, I. M., Gunn, S., Pascal, R., Matei, A., and Blomquist, B.: Ocean bubbles under high wind conditions – Part 1: Bubble distribution and development, Ocean Sci., 18, 565–586, https://doi.org/10.5194/os-18-565-2022, 2022.

Dacey, J. W. and Wakeham, S. G.: Oceanic dimethylsulfide: production during zooplankton grazing on phytoplankton, Science, 233, 1314–1316, 1986.

Dall'Osto, M., Vaqué, D., Sotomayor-Garcia, A., Cabrera-Brufau, M., Estrada, M., Buchaca, T., Soler, M., Nunes, S., Zeppenfeld, S., Van Pinxteren, M., Herrmann, H., Wex, H., Rinaldi, M., Paglione, M., Beddows, D. C. S., Harrison, R. M., and Berdalet, E.: Sea Ice Microbiota in the Antarctic Peninsula Modulates Cloud-Relevant Sea Spray Aerosol Production, Front. Mar. Sci., 9, 827061, https://doi.org/10.3389/fmars.2022.827061, 2022.

Dall'Osto, M., Schmidt, K., Campbell, R. G., Nomura, D., Park, J., Yoon, Y. J., and Park, J.: Zooplankton grazing increases atmospheric primary aerosol production in the high Arctic, Elem Sci Anth, 13, 00078, https://doi.org/10.1525/elementa.2024.00078, 2025.

https://doi.org/10.5194/egusphere-2026-2745
Preprint. Discussion started: 27 May 2026

Dani, K. G. S. and Loreto, F.: Trade-Off Between Dimethyl Sulfide and Isoprene Emissions from Marine Phytoplankton, Trends in Plant Science, 22, 361–372, https://doi.org/10.1016/j.tplants.2017.01.006, 2017.

DeCarlo, P. F., Kimmel, J. R., Trimborn, A., Northway, M. J., Jayne, J. T., Aiken, A. C., Gonin, M., Fuhrer, K., Horvath, T., Docherty, K. S., Worsnop, D. R., and Jimenez, J. L.: Field-Deployable, High-Resolution, Time-of-Flight Aerosol Mass Spectrometer, Anal. Chem., 78, 8281–8289, https://doi.org/10.1021/ac061249n, 2006.

Demory, D., Weitz, J. S., Baudoux, A., Touzeau, S., Simon, N., Rabouille, S., Sciandra, A., and Bernard, O.: A thermal trade-off between viral production and degradation drives virus-phytoplankton population dynamics, Ecology Letters, 24, 1133–1144, https://doi.org/10.1111/ele.13722, 2021.

Drewnick, F., Hings, S. S., Alfarra, M. R., Prevot, A. S. H., and Borrmann, S.: Aerosol quantification with the Aerodyne Aerosol Mass Spectrometer: detection limits and ionizer background effects, Atmos. Meas. Tech., 2, 33–46, https://doi.org/10.5194/amt-2-33-2009, 2009.

Duhamel, S., Kim, E., Sprung, B., and Anderson, O. R.: Small pigmented eukaryotes play a major role in carbon cycling in the P-depleted western subtropical North Atlantic, which may be supported by mixotrophy, Limnology & Oceanography, 64, 2424–2440, https://doi.org/10.1002/lno.11193, 2019a.

Duhamel, S., Kim, E., Sprung, B., and Anderson, O. R.: Small pigmented eukaryotes play a major role in carbon cycling in the P-depleted western subtropical North Atlantic, which may be supported by mixotrophy, Limnology & Oceanography, 64, 2424–2440, https://doi.org/10.1002/lno.11193, 2019b.

Efron, B.: Bootstrap Methods: Another Look at the Jackknife, The Annals of Statistics, 7, 1–26, 1979.

Eickhoff, L., Bayer-Giraldi, M., Reicher, N., Rudich, Y., and Koop, T.: Ice nucleating properties of the sea ice diatom *Fragilariopsis cylindrus* and its exudates, Biogeosciences, 20, 1–14, https://doi.org/10.5194/bg-20-1-2023, 2023.

Eigemann, F., Tait, K., Temperton, B., and Hellweger, F. L.: Internal carbon recycling by heterotrophic prokaryotes compensates for mismatches between phytoplankton production and heterotrophic consumption, The ISME Journal, 18, wrae103, https://doi.org/10.1093/ismejo/wrae103, 2024.

European Union-Copernicus Marine Service: Global ocean low and mid trophic levels biomass content hindcast, https://doi.org/10.48670/MOI-00020, 2021.

Fiddes, S. L., Woodhouse, M. T., Nicholls, Z., Lane, T. P., and Schofield, R.: Cloud, precipitation and radiation responses to large perturbations in global dimethyl sulfide, Atmos. Chem. Phys., 18, 10177–10198, https://doi.org/10.5194/acp-18-10177-2018, 2018.

https://doi.org/10.5194/egusphere-2026-2745
Preprint. Discussion started: 27 May 2026

Forster, P. M., Smith, C. J., Walsh, T., Lamb, W. F., Lamboll, R., Hauser, M., Ribes, A., Rosen, D., Gillett, N., Palmer, M. D., Rogelj, J., Von Schuckmann, K., Seneviratne, S. I., Trewin, B., Zhang, X., Allen, M., Andrew, R., Birt, A., Borger, A., Boyer, T., Broersma, J. A., Cheng, L., Dentener, F., Friedlingstein, P., Gutiérrez, J. M., Gütschow, J., Hall, B., Ishii, M., Jenkins, S., Lan, X., Lee, J.-Y., Morice, C., Kadow, C., Kennedy, J., Killick, R., Minx, J. C., Naik, V., Peters, G. P., Pirani, A., Pongratz, J., Schleussner, C.-F., Szopa, S., Thorne, P., Rohde, R., Rojas Corradi, M., Schumacher, D., Vose, R., Zickfeld, K., Masson-Delmotte, V., and Zhai, P.: Indicators of Global Climate Change 2022: annual update of large-scale indicators of the state of the climate system and human influence, Earth Syst. Sci. Data, 15, 2295–2327, https://doi.org/10.5194/essd-15-2295-2023, 2023.

Fossum, K. N., Lin, C., O'Sullivan, N., Lei, L., Hellebust, S., Ceburnis, D., Afzal, A., Tremper, A., Green, D., Jain, S., Byčenkienė, S., O'Dowd, C., Wenger, J., and Ovadnevaite, J.: Two distinct ship emission profiles for organic-sulfate source apportionment of PM in sulfur emission control areas, Atmos. Chem. Phys., 24, 10815–10831, https://doi.org/10.5194/acp-24-10815-2024, 2024.

Freney, E., Sellegri, K., Nicosia, A., Trueblood, J. T., Rinaldi, M., Williams, L. R., Prévôt, A. S. H., Thyssen, M., Grégori, G., Haëntjens, N., Dinasquet, J., Obernosterer, I., Van-Wambeke, F., Engel, A., Zäncker, B., Desboeufs, K., Asmi, E., Timmonen, H., and Guieu, C.: Mediterranean nascent sea spray organic aerosol and relationships with seawater biogeochemistry, Aerosols/Field Measurements/Troposphere/Chemistry (chemical composition and reactions), https://doi.org/10.5194/acp-2020-406, 2020.

Fulton, J. M., Fredricks, H. F., Bidle, K. D., Vardi, A., Kendrick, B. J., DiTullio, G. R., and Van Mooy, B. A. S.: Novel molecular determinants of viral susceptibility and resistance in the lipidome of *E miliania huxleyi*, Environmental Microbiology, 16, 1137–1149, https://doi.org/10.1111/1462-2920.12358, 2014.

Fung, K. M., Heald, C. L., Kroll, J. H., Wang, S., Jo, D. S., Gettelman, A., Lu, Z., Liu, X., Zaveri, R. A., Apel, E., Blake, D. R., Jimenez, J.-L., Campuzano-Jost, P., Veres, P., Bates, T. S., Shilling, J. E., and Zawadowicz, M.: Exploring DMS oxidation and implications for global aerosol radiative forcing, Aerosols/Atmospheric Modelling/Troposphere/Chemistry (chemical composition and reactions), https://doi.org/10.5194/acp-2021-782, 2021.

Gangrade, S. and Mangolte, I.: Patchiness of plankton communities at fronts explained by Lagrangian history of upwelled water parcels, Limnology & Oceanography, 69, 2123–2137, https://doi.org/10.1002/lno.12654, 2024.

https://doi.org/10.5194/egusphere-2026-2745
Preprint. Discussion started: 27 May 2026

Giannerini, S. and Goracci, G.: Entropy-Based Tests for Complex Dependence in Economic and Financial Time Series with the R Package tseriesEntropy, Mathematics, 11, 757, https://doi.org/10.3390/math11030757, 2023a.

Giannerini, S. and Goracci, G.: Entropy-Based Tests for Complex Dependence in Economic and Financial Time Series with the R Package tseriesEntropy, Mathematics, 11, 757, https://doi.org/10.3390/math11030757, 2023b.

Goss, M. B. and Kroll, J. H.: Chamber studies of OH + dimethyl sulfoxide and dimethyl disulfide: insights into the dimethyl sulfide oxidation mechanism, Atmos. Chem. Phys., 24, 1299–1314, https://doi.org/10.5194/acp-24-1299-2024, 2024.

Gouhier, T., Grinsted, A., and Simko, V.: biwavelet: Conduct Univariate and Bivariate Wavelet Analyses, https://doi.org/10.32614/CRAN.package.biwavelet, 2012.

Gray, P. C., Savelyev, I., Cassar, N., Lévy, M., Boss, E., Lehahn, Y., Bourdin, G., Thompson, K. A., Windle, A., Gronniger, J., Floge, S., Hunt, D. E., Silsbe, G., Johnson, Z. I., and Johnston, D. W.: Evidence for Kilometer-Scale Biophysical Features at the Gulf Stream Front, JGR Oceans, 129, e2023JC020526, https://doi.org/10.1029/2023JC020526, 2024.

Grigas, T., Ovadnevaite, J., Ceburnis, D., Moran, E., McGovern, F. M., Jennings, S. G., and O'Dowd, C.: Sophisticated Clean Air Strategies Required to Mitigate Against Particulate Organic Pollution, Sci Rep, 7, 44737, https://doi.org/10.1038/srep44737, 2017.

Gu, W., Xie, Z., Wei, Z., Chen, A., Jiang, B., Yue, F., and Yu, X.: Marine Fresh Carbon Pool Dominates Summer Carbonaceous Aerosols Over Arctic Ocean, JGR Atmospheres, 128, e2022JD037692, https://doi.org/10.1029/2022JD037692, 2023.

Guadayol, Ò., Mendonca, T., Segura-Noguera, M., Wright, A. J., Tassieri, M., and Humphries, S.: Microrheology reveals microscale viscosity gradients in planktonic systems, Proc. Natl. Acad. Sci. U.S.A., 118, e2011389118, https://doi.org/10.1073/pnas.2011389118, 2021.

Hansell, D. A., Romera-Castillo, C., and Lopez, C. N.: Dynamics of dissolved organic carbon in the global ocean, in: Biogeochemistry of Marine Dissolved Organic Matter, Elsevier, 769–802, https://doi.org/10.1016/B978-0-443-13858-4.00004-6, 2024.

Hodshire, A. L., Campuzano-Jost, P., Kodros, J. K., Croft, B., Nault, B. A., Schroder, J. C., Jimenez, J. L., and Pierce, J. R.: The potential role of methanesulfonic acid (MSA) in aerosol formation and growth and the

https://doi.org/10.5194/egusphere-2026-2745
Preprint. Discussion started: 27 May 2026

associated radiative forcings, Atmos. Chem. Phys., 19, 3137–3160, https://doi.org/10.5194/acp-19-3137-2019, 2019.

Holm, H. C., Fredricks, H. F., Bent, S. M., Lowenstein, D. P., Ossolinski, J. E., Becker, K. W., Johnson, W. M., Schrage, K., and Van Mooy, B. A. S.: Global ocean lipidomes show a universal relationship between temperature and lipid unsaturation, Science, 376, 1487–1491, https://doi.org/10.1126/science.abn7455, 2022.

Hong, Z., Long, D., Shan, K., Zhang, J.-M., Woolway, R. I., Liu, M., Mann, M. E., and Fang, H.: Declining ocean greenness and phytoplankton blooms in low to mid-latitudes under a warming climate, Sci. Adv., 11, eadx4857, https://doi.org/10.1126/sciadv.adx4857, 2025.

Hu, J., Li, J., Tsona Tchinda, N., Song, Y., Xu, M., Li, K., and Du, L.: Underestimated role of sea surface temperature in sea spray aerosol formation and climate effects, npj Clim Atmos Sci, 7, 273, https://doi.org/10.1038/s41612-024-00823-x, 2024.

Hulswar, S., Simó, R., Galí, M., Bell, T. G., Lana, A., Inamdar, S., Halloran, P. R., Manville, G., and Mahajan, A. S.: Third revision of the global surface seawater dimethyl sulfide climatology (DMS-Rev3), Earth Syst. Sci. Data, 14, 2963–2987, https://doi.org/10.5194/essd-14-2963-2022, 2022.

Ickes, L., Porter, G. C. E., Wagner, R., Adams, M. P., Bierbauer, S., Bertram, A. K., Bilde, M., Christiansen, S., Ekman, A. M. L., Gorokhova, E., Höhler, K., Kiselev, A. A., Leck, C., Möhler, O., Murray, B. J., Schiebel, T., Ullrich, R., and Salter, M. E.: The ice-nucleating activity of Arctic sea surface microlayer samples and marine algal cultures, Atmos. Chem. Phys., 20, 11089–11117, https://doi.org/10.5194/acp-20-11089-2020, 2020.

Jackson, R. and Gabric, A.: Climate Change Impacts on the Marine Cycling of Biogenic Sulfur: A Review, Microorganisms, 10, 1581, https://doi.org/10.3390/microorganisms10081581, 2022.

Jang, E., Park, K.-T., Yoon, Y. J., Kim, T.-W., Hong, S.-B., Becagli, S., Traversi, R., Kim, J., and Gim, Y.: New particle formation events observed at the King Sejong Station, Antarctic Peninsula – Part 2: Link with the oceanic biological activities, Atmos. Chem. Phys., 19, 7595–7608, https://doi.org/10.5194/acp-19-7595-2019, 2019.

Jung, J., Hong, S.-B., Chen, M., Hur, J., Jiao, L., Lee, Y., Park, K., Hahm, D., Choi, J.-O., Yang, E. J., Park, J., Kim, T.-W., and Lee, S.: Characteristics of methanesulfonic acid, non-sea-salt sulfate and organic carbon aerosols over the Amundsen Sea, Antarctica, Atmos. Chem. Phys., 20, 5405–5424, https://doi.org/10.5194/acp-20-5405-2020, 2020.

https://doi.org/10.5194/egusphere-2026-2745
Preprint. Discussion started: 27 May 2026

Kaluarachchi, C. P., Or, V. W., Lan, Y., Hasenecz, E. S., Kim, D., Madawala, C. K., Dorcé, G. P., Mayer, K. J., Sauer, J. S., Lee, C., Cappa, C. D., Bertram, T. H., Stone, E. A., Prather, K. A., Grassian, V. H., and Tivanski, A. V.: Effects of Atmospheric Aging Processes on Nascent Sea Spray Aerosol Physicochemical Properties, ACS Earth Space Chem., 6, 2732–2744, https://doi.org/10.1021/acsearthspacechem.2c00258, 2022.

Kawana, K., Miyazaki, Y., Omori, Y., Tanimoto, H., Kagami, S., Suzuki, K., Yamashita, Y., Nishioka, J., Deng, Y., Yai, H., and Mochida, M.: Number-Size Distribution and CCN Activity of Atmospheric Aerosols in the Western North Pacific During Spring Pre-Bloom Period: Influences of Terrestrial and Marine Sources, JGR Atmospheres, 127, e2022JD036690, https://doi.org/10.1029/2022JD036690, 2022.

Killick, R., Beaulieu, C., Taylor, S., and Hullait, H.: EnvCpt: Detection of Structural Changes in Climate and Environment Time Series, 2018.

Krisch, S., Browning, T. J., Graeve, M., Ludwichowski, K.-U., Lodeiro, P., Hopwood, M. J., Roig, S., Yong, J.-C., Kanzow, T., and Achterberg, E. P.: The influence of Arctic Fe and Atlantic fixed N on summertime primary production in Fram Strait, North Greenland Sea, Sci Rep, 10, 15230, https://doi.org/10.1038/s41598-020-72100-9, 2020.

Law, C. S. and Miller, L. A.: The air-sea interface in a changing climate: Research advances and future directions, Elem Sci Anth, 13, 00022, https://doi.org/10.1525/elementa.2025.00022, 2025.

Lawler, M. J., Schill, G. P., Brock, C. A., Froyd, K. D., Williamson, C., Kupc, A., and Murphy, D. M.: Sea Spray Aerosol Over the Remote Oceans Has Low Organic Content, AGU Advances, 5, e2024AV001215, https://doi.org/10.1029/2024AV001215, 2024.

Le Gland, G., Masdeu-Navarro, M., Galí, M., Vallina, S. M., Gralka, M., Vincent, F., Cordero, O., Vardi, A., and Simó, R.: Biological sources and sinks of dimethylsulfide disentangled by an induced bloom experiment and a numerical model, Limnology & Oceanography, 69, 140–157, https://doi.org/10.1002/lno.12470, 2024.

Leon-Marcos, A., Zeising, M., Van Pinxteren, M., Zeppenfeld, S., Bracher, A., Barbaro, E., Engel, A., Feltracco, M., Tegen, I., and Heinold, B.: Modelling emission and transport of key components of primary marine organic aerosol using the global aerosol-climate model ECHAM6.3–HAM2.3, https://doi.org/10.5194/egusphere-2024-2917, 30 September 2024.

Lima-Mendez, G., Faust, K., Henry, N., Decelle, J., Colin, S., Carcillo, F., Chaffron, S., Ignacio-Espinosa, J. C., Roux, S., Vincent, F., Bittner, L., Darzi, Y., Wang, J., Audic, S., Berline, L., Bontempi, G., Cabello, A.

https://doi.org/10.5194/egusphere-2026-2745
Preprint. Discussion started: 27 May 2026

M., Coppola, L., Cornejo-Castillo, F. M., d'Ovidio, F., De Meester, L., Ferrera, I., Garet-Delmas, M.-J., Guidi, L., Lara, E., Pesant, S., Royo-Llonch, M., Salazar, G., Sánchez, P., Sebastian, M., Souffreau, C., Dimier, C., Picheral, M., Searson, S., Kandels-Lewis, S., Tara Oceans coordinators, Gorsky, G., Not, F., Ogata, H., Speich, S., Stemmann, L., Weissenbach, J., Wincker, P., Acinas, S. G., Sunagawa, S., Bork, P., Sullivan, M. B., Karsenti, E., Bowler, C., De Vargas, C., and Raes, J.: Determinants of community structure in the global plankton interactome, Science, 348, 1262073, https://doi.org/10.1126/science.1262073, 2015.

Liu, C., Li, H., Zheng, H., Wang, G., Qin, X., Chen, J., Zhou, S., Lu, D., Liang, G., Song, X., Duan, Y., Liu, J., Huang, K., and Deng, C.: Ocean Emission Pathway and Secondary Formation Mechanism of Aminiums Over the Chinese Marginal Sea, JGR Atmospheres, 127, e2022JD037805, https://doi.org/10.1029/2022JD037805, 2022.

Liu, W., Holm, H. C., Lipp, J. S., Fredricks, H. F., Van Mooy, B. A. S., and Hinrichs, K.-U.: Unraveling plankton adaptation in global oceans through the untargeted analysis of lipidomes, Sci. Adv., 11, eads4605, https://doi.org/10.1126/sciadv.ads4605, 2025a.

Liu, X. and Wang, M.: Global daily gap-free ocean color products from multi-satellite measurements, International Journal of Applied Earth Observation and Geoinformation, 108, 102714, https://doi.org/10.1016/j.jag.2022.102714, 2022.

Liu, Y., Yu, L., Yao, Z., Shen, Y., and Pan, Y.: The effects of turbulence on the growth of three different diatom species, Front. Mar. Sci., 11, 1400798, https://doi.org/10.3389/fmars.2024.1400798, 2024.

Liu, Y., He, Q., Zhan, W., Guo, M., Zheng, Y., Shen, X., and Zhan, H.: Heterogeneity of phytoplankton response to submesoscale processes in the global ocean, Commun Earth Environ, 6, 386, https://doi.org/10.1038/s43247-025-02365-3, 2025b.

Longhurst, A. R.: Ecological geography of the sea, Elsevier, 2010.

Lowenstein, D., Holm, H., Fredricks, H., and Mooy, B. V.: Lipid stoichiometry and biomarkers reflect microbial acclimation and nutrient stress across the Atlantic Ocean, https://doi.org/10.21203/rs.3.rs-8022751/v1, 19 November 2025.

Lu, Z., Qin, G., Zheng, L., Zhang, Y., Huang, L., Zhou, J., Liu, Y., Zheng, M., Hou, E., Song, L., Liu, H., Jiao, N., and Wang, F.: The role of phytoplankton in structuring global oceanic dissolved organic carbon pools, Nat Commun, 16, 7742, https://doi.org/10.1038/s41467-025-63105-x, 2025.

https://doi.org/10.5194/egusphere-2026-2745
Preprint. Discussion started: 27 May 2026

Malfatti, F., Lee, C., Tinta, T., Pendergraft, M. A., Celussi, M., Zhou, Y., Sultana, C. M., Rotter, A., Axson, J. L., Collins, D. B., Santander, M. V., Anides Morales, A. L., Aluwihare, L. I., Riemer, N., Grassian, V. H., Azam, F., and Prather, K. A.: Detection of Active Microbial Enzymes in Nascent Sea Spray Aerosol: Implications for Atmospheric Chemistry and Climate, Environ. Sci. Technol. Lett., 6, 171–177, https://doi.org/10.1021/acs.estlett.8b00699, 2019.

Malitsky, S., Ziv, C., Rosenwasser, S., Zheng, S., Schatz, D., Porat, Z., Ben-Dor, S., Aharoni, A., and Vardi, A.: Viral infection of the marine alga *Emiliania huxleyi* triggers lipidome remodeling and induces the production of highly saturated triacylglycerol, New Phytologist, 210, 88–96, https://doi.org/10.1111/nph.13852, 2016.

Mansour, K., Decesari, S., Ceburnis, D., Ovadnevaite, J., Russell, L. M., Paglione, M., Poulain, L., Huang, S., O'Dowd, C., and Rinaldi, M.: IPB-MSA&SO_4 : a daily 0.25° resolution dataset of in situ-produced biogenic methanesulfonic acid and sulfate over the North Atlantic during 1998–2022 based on machine learning, Earth Syst. Sci. Data, 16, 2717–2740, https://doi.org/10.5194/essd-16-2717-2024, 2024.

Markuszewski, P., Nilsson, E. D., Zinke, J., Mårtensson, E. M., Salter, M., Makuch, P., Kitowska, M., Niedźwiecka-Wróbel, I., Drozdowska, V., Lis, D., Petelski, T., Ferrero, L., and Piskozub, J.: Multi-year gradient measurements of sea spray fluxes over the Baltic Sea and the North Atlantic Ocean, https://doi.org/10.5194/egusphere-2024-1254, 3 June 2024.

Martínez-Pérez, C., Zweifel, S. T., Pioli, R., and Stocker, R.: Space, the final frontier: The spatial component of phytoplankton–bacterial interactions, Molecular Microbiology, 122, 331–346, https://doi.org/10.1111/mmi.15293, 2024.

Middlebrook, A. M., Bahreini, R., Jimenez, J. L., and Canagaratna, M. R.: Evaluation of Composition-Dependent Collection Efficiencies for the Aerodyne Aerosol Mass Spectrometer using Field Data, Aerosol Science and Technology, 46, 258–271, https://doi.org/10.1080/02786826.2011.620041, 2012.

Moallemi, A., Landwehr, S., Robinson, C., Simó, R., Zamanillo, M., Chen, G., Baccarini, A., Schnaiter, M., Henning, S., Modini, R. L., Gysel-Beer, M., and Schmale, J.: Sources, Occurrence and Characteristics of Fluorescent Biological Aerosol Particles Measured Over the Pristine Southern Ocean, JGR Atmospheres, 126, e2021JD034811, https://doi.org/10.1029/2021JD034811, 2021.

Mojica, K. D. A., Huisman, J., Wilhelm, S. W., and Brussaard, C. P. D.: Latitudinal variation in virus-induced mortality of phytoplankton across the North Atlantic Ocean, The ISME Journal, 10, 500–513, https://doi.org/10.1038/ismej.2015.130, 2016.

https://doi.org/10.5194/egusphere-2026-2745
Preprint. Discussion started: 27 May 2026

Moritz, S. and Bartz-Beielstein, T.: imputeTS: Time Series Missing Value Imputation in R, The R Journal, 9, 207–218, https://doi.org/10.32614/RJ-2017-009, 2017.

Moschos, V., Chevassus, E., Fossum, K., Lei, L., Pernov, J., Humphries, R., Keywood, M., O'Dowd, C., Ceburnis, D., and Ovadnevaite, J.: Rising natural aerosols drive marine radiative forcing as pollution declines, https://doi.org/10.21203/rs.3.rs-8776460/v1, 4 March 2026.

Needham, D. M. and Fuhrman, J. A.: Pronounced daily succession of phytoplankton, archaea and bacteria following a spring bloom, Nat Microbiol, 1, 16005, https://doi.org/10.1038/nmicrobiol.2016.5, 2016.

O'Dowd, C., Ceburnis, D., Ovadnevaite, J., Vaishya, A., Rinaldi, M., and Facchini, M. C.: Do anthropogenic, continental or coastal aerosol sources impact on a marine aerosol signature at Mace Head?, Atmos. Chem. Phys., 14, 10687–10704, https://doi.org/10.5194/acp-14-10687-2014, 2014.

O'Dowd, C., Ceburnis, D., Ovadnevaite, J., Bialek, J., Stengel, D. B., Zacharias, M., Nitschke, U., Connan, S., Rinaldi, M., Fuzzi, S., Decesari, S., Cristina Facchini, M., Marullo, S., Santoleri, R., Dell'Anno, A., Corinaldesi, C., Tangherlini, M., and Danovaro, R.: Connecting marine productivity to sea-spray via nanoscale biological processes: Phytoplankton Dance or Death Disco?, Sci Rep, 5, 14883, https://doi.org/10.1038/srep14883, 2015.

O'Dowd, C. D., Facchini, M. C., Cavalli, F., Ceburnis, D., Mircea, M., Decesari, S., Fuzzi, S., Yoon, Y. J., and Putaud, J.-P.: Biogenically driven organic contribution to marine aerosol, Nature, 431, 676–680, https://doi.org/10.1038/nature02959, 2004.

Ovadnevaite, J., O'Dowd, C., Dall'Osto, M., Ceburnis, D., Worsnop, D. R., and Berresheim, H.: Detecting high contributions of primary organic matter to marine aerosol: A case study, Geophysical Research Letters, 38, https://doi.org/10.1029/2010GL046083, 2011a.

Ovadnevaite, J., O'Dowd, C., Dall'Osto, M., Ceburnis, D., Worsnop, D. R., and Berresheim, H.: Detecting high contributions of primary organic matter to marine aerosol: A case study: PRIMARY ORGANIC MARINE AEROSOL, Geophys. Res. Lett., 38, n/a-n/a, https://doi.org/10.1029/2010GL046083, 2011b.

Ovadnevaite, J., Ceburnis, D., Martucci, G., Bialek, J., Monahan, C., Rinaldi, M., Facchini, M. C., Berresheim, H., Worsnop, D. R., and O'Dowd, C.: Primary marine organic aerosol: A dichotomy of low hygroscopicity and high CCN activity: MARINE AEROSOL-CLOUD INTERACTIONS, Geophys. Res. Lett., 38, n/a-n/a, https://doi.org/10.1029/2011GL048869, 2011c.

https://doi.org/10.5194/egusphere-2026-2745
Preprint. Discussion started: 27 May 2026

Ovadnevaite, J., Manders, A., de Leeuw, G., Ceburnis, D., Monahan, C., Partanen, A.-I., Korhonen, H., and O'Dowd, C. D.: A sea spray aerosol flux parameterization encapsulating wave state, Atmos. Chem. Phys., 14, 1837–1852, https://doi.org/10.5194/acp-14-1837-2014, 2014a.

Ovadnevaite, J., Ceburnis, D., Leinert, S., Dall'Osto, M., Canagaratna, M., O'Doherty, S., Berresheim, H., and O'Dowd, C.: Submicron NE Atlantic marine aerosol chemical composition and abundance: Seasonal trends and air mass categorization: Seasonal Trends of Marine Aerosol, J. Geophys. Res. Atmos., 119, 11,850-11,863, https://doi.org/10.1002/2013JD021330, 2014b.

Ovadnevaite, J., Zuend, A., Laaksonen, A., Sanchez, K. J., Roberts, G., Ceburnis, D., Decesari, S., Rinaldi, M., Hodas, N., Facchini, M. C., Seinfeld, J. H., and O' Dowd, C.: Surface tension prevails over solute effect in organic-influenced cloud droplet activation, Nature, 546, 637–641, https://doi.org/10.1038/nature22806, 2017.

Owen, K., Saeki, K., Warren, J. D., Bocconcelli, A., Wiley, D. N., Ohira, S.-I., Bombosch, A., Toda, K., and Zitterbart, D. P.: Natural dimethyl sulfide gradients would lead marine predators to higher prey biomass, Commun Biol, 4, 149, https://doi.org/10.1038/s42003-021-01668-3, 2021.

Partanen, A.-I., Dunne, E. M., Bergman, T., Laakso, A., Kokkola, H., Ovadnevaite, J., Sogacheva, L., Baisnée, D., Sciare, J., Manders, A., O'Dowd, C., De Leeuw, G., and Korhonen, H.: Global modelling of direct and indirect effects of sea spray aerosol using a source function encapsulating wave state, Atmos. Chem. Phys., 14, 11731–11752, https://doi.org/10.5194/acp-14-11731-2014, 2014.

Pierella Karlusich, J. J., Cosnier, K., Zinger, L., Henry, N., Nef, C., Bernard, G., Scalco, E., Dvorak, E., Tara Oceans Coordinators, Acinas, S. G., Babin, M., Bork, P., Boss, E., Bowler, C., Cochrane, G., De Vargas, C., Gorsky, G., Grimsley, N., Guidi, L., Iudicone, D., Jaillon, O., Kandels, S., Karp-Boss, L., Karsenti, E., Not, F., Ogata, H., Pesant, S., Poulton, N., Sardet, C., Speich, S., Stemmann, L., Sullivan, M. B., Sunagawa, S., Wincker, P., Rocha Jimenez Vieira, F., Delage, E., Chaffron, S., Ovchinnikov, S., Zingone, A., and Bowler, C.: Patterns and drivers of diatom diversity and abundance in the global ocean, Nat Commun, 16, https://doi.org/10.1038/s41467-025-58027-7, 2025.

Prochaska, J. X. and Frouin, R. J.: On the Peril of Inferring Phytoplankton Properties from Remote-Sensing Observations, https://doi.org/10.48550/ARXIV.2408.06149, 2024.

Rahlff, J., Stolle, C., Giebel, H.-A., Brinkhoff, T., Ribas-Ribas, M., Hodapp, D., and Wurl, O.: High wind speeds prevent formation of a distinct bacterioneuston community in the sea-surface microlayer, FEMS Microbiology Ecology, 93, https://doi.org/10.1093/femsec/fix041, 2017.

https://doi.org/10.5194/egusphere-2026-2745
Preprint. Discussion started: 27 May 2026

Roesler, C., Uitz, J., Claustre, H., Boss, E., Xing, X., Organelli, E., Briggs, N., Bricaud, A., Schmechtig, C., Poteau, A., D'Ortenzio, F., Ras, J., Drapeau, S., Haëntjens, N., and Barbieux, M.: Recommendations for obtaining unbiased chlorophyll estimates from in situ chlorophyll fluorometers: A global analysis of WET Labs ECO sensors, Limnology & Ocean Methods, 15, 572–585, https://doi.org/10.1002/lom3.10185, 2017.

Rosati, B., Isokääntä, S., Christiansen, S., Jensen, M. M., Moosakutty, S. P., Wollesen De Jonge, R., Massling, A., Glasius, M., Elm, J., Virtanen, A., and Bilde, M.: Hygroscopicity and CCN potential of DMS derived aerosol particles, https://doi.org/10.5194/acp-2022-188, 29 March 2022.

Rosenwasser, S., Mausz, M. A., Schatz, D., Sheyn, U., Malitsky, S., Aharoni, A., Weinstock, E., Tzfadia, O., Ben-Dor, S., Feldmesser, E., Pohnert, G., and Vardi, A.: Rewiring Host Lipid Metabolism by Large Viruses Determines the Fate of *Emiliania huxleyi* , a Bloom-Forming Alga in the Ocean, The Plant Cell, 26, 2689–2707, https://doi.org/10.1105/tpc.114.125641, 2014.

Schwier, A. N., Rose, C., Asmi, E., Ebling, A. M., Landing, W. M., Marro, S., Pedrotti, M.-L., Sallon, A., Iuculano, F., Agusti, S., Tsiola, A., Pitta, P., Louis, J., Guieu, C., Gazeau, F., and Sellegri, K.: Primary marine aerosol emissions from the Mediterranean Sea during pre-bloom and oligotrophic conditions: correlations to seawater chlorophyll *a* from a mesocosm study, Atmos. Chem. Phys., 15, 7961–7976, https://doi.org/10.5194/acp-15-7961-2015, 2015.

Schwier, A. N., Sellegri, K., Mas, S., Charrière, B., Pey, J., Rose, C., Temime-Roussel, B., Jaffrezo, J.-L., Parin, D., Picard, D., Ribeiro, M., Roberts, G., Sempéré, R., Marchand, N., and D'Anna, B.: Primary marine aerosol physical flux and chemical composition during a nutrient enrichment experiment in mesocosms in the Mediterranean Sea, Atmos. Chem. Phys., 17, 14645–14660, https://doi.org/10.5194/acp-17-14645-2017, 2017.

Seidel, M., Vemulapalli, S. P. B., Mathieu, D., and Dittmar, T.: Marine Dissolved Organic Matter Shares Thousands of Molecular Formulae Yet Differs Structurally across Major Water Masses, Environ. Sci. Technol., 56, 3758–3769, https://doi.org/10.1021/acs.est.1c04566, 2022.

Selden, C. R., LaBrie, R., Ganley, L. C., Crocker, D. R., Peleg, O., Perry, D. C., Reich, H. G., Sasaki, M., Thibodeau, P. S., and Isanta-Navarro, J.: Is our understanding of aquatic ecosystems sufficient to quantify ecologically driven climate feedbacks?, Global Change Biology, 30, e17351, https://doi.org/10.1111/gcb.17351, 2024.

https://doi.org/10.5194/egusphere-2026-2745
Preprint. Discussion started: 27 May 2026

Sellegri, K., Nicosia, A., Freney, E., Uitz, J., Thyssen, M., Grégori, G., Engel, A., Zäncker, B., Haëntjens, N., Mas, S., Picard, D., Saint-Macary, A., Peltola, M., Rose, C., Trueblood, J., Lefevre, D., D'Anna, B., Desboeufs, K., Meskhidze, N., Guieu, C., and Law, C. S.: Surface ocean microbiota determine cloud precursors, Sci Rep, 11, 281, https://doi.org/10.1038/s41598-020-78097-5, 2021.

Sellegri, K., Barthelmeß, T., Trueblood, J., Cristi, A., Freney, E., Rose, C., Barr, N., Harvey, M., Safi, K., Deppeler, S., Thompson, K., Dillon, W., Engel, A., and Law, C.: Quantified effect of seawater biogeochemistry on the temperature dependence of sea spray aerosol fluxes, Atmos. Chem. Phys., 23, 12949–12964, https://doi.org/10.5194/acp-23-12949-2023, 2023.

Sellegri, K., Simó, R., Wang, B., Alpert, P. A., Altieri, K., Burrows, S., Hopkins, F. E., Koren, I., McCoy, I. L., Ovadnevaite, J., Salter, M., and Schmale, J.: Influence of open ocean biogeochemistry on aerosol and clouds: Recent findings and perspectives, Elem Sci Anth, 12, 00058, https://doi.org/10.1525/elementa.2023.00058, 2024.

Shemi, A., Ben-Dor, S., Rotkopf, R., Dym, O., and Vardi, A.: Phylogeny and biogeography of the algal DMS-releasing enzyme in the global ocean, ISME Communications, 3, https://doi.org/10.1038/s43705-023-00280-2, 2023.

Simis, S. G. H., Ruiz-Verdú, A., Domínguez-Gómez, J. A., Peña-Martinez, R., Peters, S. W. M., and Gons, H. J.: Influence of phytoplankton pigment composition on remote sensing of cyanobacterial biomass, Remote Sensing of Environment, 106, 414–427, https://doi.org/10.1016/j.rse.2006.09.008, 2007.

Simon, L., Favez, O., Petit, J.-E., Canonaco, F., Slowik, J. G., Marchand, C., and Gros, V.: Source apportionment of organic gaseous and particulate compounds using a combined positive matrix factorization approach in summer (2020) in the Paris region (France), Atmospheric Environment, 354, 121269, https://doi.org/10.1016/j.atmosenv.2025.121269, 2025.

Stein, A. F., Draxler, R. R., Rolph, G. D., Stunder, B. J. B., Cohen, M. D., and Ngan, F.: NOAA's HYSPLIT Atmospheric Transport and Dispersion Modeling System, Bulletin of the American Meteorological Society, 96, 2059–2077, https://doi.org/10.1175/BAMS-D-14-00110.1, 2015.

Swan, C. M., Vogt, M., Gruber, N., and Laufkoetter, C.: A global seasonal surface ocean climatology of phytoplankton types based on CHEMTAX analysis of HPLC pigments, Deep Sea Research Part I: Oceanographic Research Papers, 109, 137–156, https://doi.org/10.1016/j.dsr.2015.12.002, 2016.

https://doi.org/10.5194/egusphere-2026-2745
Preprint. Discussion started: 27 May 2026

Taipale, S., Peltomaa, E., and Salmi, P.: Variation in ω-3 and ω-6 Polyunsaturated Fatty Acids Produced by Different Phytoplankton Taxa at Early and Late Growth Phase, Biomolecules, 10, 559, https://doi.org/10.3390/biom10040559, 2020.

Thibault, H., Ménard, F., Abitbol-Spangaro, J., Poggiale, J.-C., and Martini, S.: Modeling the contribution of micronekton diel vertical migrations to carbon export in the mesopelagic zone, Biogeosciences, 22, 2181–2200, https://doi.org/10.5194/bg-22-2181-2025, 2025.

Thornton, D. C. O., Brooks, S. D., Wilbourn, E. K., Mirrielees, J., Alsante, A. N., Gold-Bouchot, G., Whitesell, A., and Kiana McFadden, K.: Production of aerosol containing ice nucleating particles (INPs) by fast growing phytoplankton, Aerosols/Laboratory Studies/Troposphere/Chemistry (chemical composition and reactions), https://doi.org/10.5194/acp-2022-806, 2023a.

Thornton, D. C. O., Brooks, S. D., Wilbourn, E. K., Mirrielees, J., Alsante, A. N., Gold-Bouchot, G., Whitesell, A., and McFadden, K.: Production of ice-nucleating particles (INPs) by fast-growing phytoplankton, Atmos. Chem. Phys., 23, 12707–12729, https://doi.org/10.5194/acp-23-12707-2023, 2023b.

Trueblood, J. V., Nicosia, A., Engel, A., Zäncker, B., Rinaldi, M., Freney, E., Thyssen, M., Obernosterer, I., Dinasquet, J., Belosi, F., Tovar-Sánchez, A., Rodriguez-Romero, A., Santachiara, G., Gueiu, C., and Sellegri, K.: A two-component parameterization of marine ice-nucleating particles based on seawater biology and sea spray aerosol measurements in the Mediterranean Sea, Atmos. Chem. Phys., 21, 4659–4676, https://doi.org/10.5194/acp-21-4659-2021, 2021.

Villermaux, E., Wang, X., and Deike, L.: Bubbles spray aerosols: Certitudes and mysteries, PNAS Nexus, 1, pgac261, https://doi.org/10.1093/pnasnexus/pgac261, 2022.

Wang, J., Curson, A. R. J., Zhou, S., Carrión, O., Liu, J., Vieira, A. R., Walsham, K. S., Monaco, S., Li, C.-Y., Dong, Q.-Y., Wang, Y., Rivera, P. P. L., Wang, X.-D., Zhang, M., Hanwell, L., Wallace, M., Zhu, X.-Y., Leão, P. N., Lea-Smith, D. J., Zhang, Y.-Z., Zhang, X.-H., and Todd, J. D.: Alternative dimethylsulfoniopropionate biosynthesis enzymes in diverse and abundant microorganisms, Nat Microbiol, 9, 1979–1992, https://doi.org/10.1038/s41564-024-01715-9, 2024.

Wang, S., Tang, W., Delage, E., Gifford, S., Whitby, H., González, A. G., Eveillard, D., Planquette, H., and Cassar, N.: Investigating the microbial ecology of coastal hotspots of marine nitrogen fixation in the western North Atlantic, Sci Rep, 11, 5508, https://doi.org/10.1038/s41598-021-84969-1, 2021.

https://doi.org/10.5194/egusphere-2026-2745
Preprint. Discussion started: 27 May 2026

Wenley, J., Currie, K., Lockwood, S., Thomson, B., Baltar, F., and Morales, S. E.: Seasonal Prokaryotic Community Linkages Between Surface and Deep Ocean Water, Front. Mar. Sci., 8, 659641, https://doi.org/10.3389/fmars.2021.659641, 2021.

Wieber, C., Jensen, L. Z., Vergeynst, L., Meire, L., Juul-Pedersen, T., Finster, K., and Šantl-Temkiv, T.: Terrestrial runoff is an important source of biological ice-nucleating particles in Arctic marine systems, Atmos. Chem. Phys., 25, 3327–3346, https://doi.org/10.5194/acp-25-3327-2025, 2025.

Wolf, K. K. E., Hoppe, C. J. M., Rehder, L., Schaum, E., John, U., and Rost, B.: Heatwave responses of Arctic phytoplankton communities are driven by combined impacts of warming and cooling, Sci. Adv., 10, eadl5904, https://doi.org/10.1126/sciadv.adl5904, 2024.

Wolf, M. J., Coe, A., Dove, L. A., Zawadowicz, M. A., Dooley, K., Biller, S. J., Zhang, Y., Chisholm, S. W., and Cziczo, D. J.: Investigating the Heterogeneous Ice Nucleation of Sea Spray Aerosols Using *Prochlorococcus* as a Model Source of Marine Organic Matter, Environ. Sci. Technol., 53, 1139–1149, https://doi.org/10.1021/acs.est.8b05150, 2019.

Wollesen de Jonge, R., Elm, J., Rosati, B., Christiansen, S., Hyttinen, N., Lüdemann, D., Bilde, M., and Roldin, P.: Secondary aerosol formation from dimethyl sulfide – improved mechanistic understanding based on smog chamber experiments and modelling, Atmos. Chem. Phys., 21, 9955–9976, https://doi.org/10.5194/acp-21-9955-2021, 2021.

Xu, W., Lambe, A., Silva, P., Hu, W., Onasch, T., Williams, L., Croteau, P., Zhang, X., Renbaum-Wolff, L., Fortner, E., Jimenez, J. L., Jayne, J., Worsnop, D., and Canagaratna, M.: Laboratory evaluation of species-dependent relative ionization efficiencies in the Aerodyne Aerosol Mass Spectrometer, null, 52, 626–641, https://doi.org/10.1080/02786826.2018.1439570, 2018.

Xu, W., Ovadnevaite, J., Fossum, K. N., Lin, C., Huang, R.-J., O'Dowd, C., and Ceburnis, D.: Aerosol hygroscopicity and its link to chemical composition in the coastal atmosphere of Mace Head: marine and continental air masses, Atmos. Chem. Phys., 20, 3777–3791, https://doi.org/10.5194/acp-20-3777-2020, 2020.

Xu, W., Ovadnevaite, J., Fossum, K. N., Lin, C., Huang, R.-J., Ceburnis, D., and O'Dowd, C.: Sea spray as an obscured source for marine cloud nuclei, Nat. Geosci., 15, 282–286, https://doi.org/10.1038/s41561-022-00917-2, 2022.

https://doi.org/10.5194/egusphere-2026-2745
Preprint. Discussion started: 27 May 2026

Yan, S., Xu, G., Zhang, H., Wang, J., Xu, F., Gao, X., Zhang, J., Wu, J., and Yang, G.: Factors Controlling DMS Emission and Atmospheric Sulfate Aerosols in the Western Pacific Continental Sea, JGR Oceans, 129, e2024JC020886, https://doi.org/10.1029/2024JC020886, 2024.

Zamanillo, M., Ortega-Retuerta, E., Nunes, S., Rodríguez-Ros, P., Dall'Osto, M., Estrada, M., Montserrat Sala, M., and Simó, R.: Main drivers of transparent exopolymer particle distribution across the surface Atlantic Ocean, Biogeosciences, 16, 733–749, https://doi.org/10.5194/bg-16-733-2019, 2019.

Zhang, Y., Shen, F., Li, R., Li, M., Li, Z., Chen, S., and Sun, X.: AIGD-PFT: the first AI-driven global daily gap-free 4 km phytoplankton functional type data product from 1998 to 2023, Earth Syst. Sci. Data, 16, 4793–4816, https://doi.org/10.5194/essd-16-4793-2024, 2024.

Zhou, C., Zhou, H., Holsen, T. M., Hopke, P. K., Edgerton, E. S., and Schwab, J. J.: Ambient Ammonia Concentrations Across New York State, JGR Atmospheres, 124, 8287–8302, https://doi.org/10.1029/2019JD030380, 2019.